SLAC-PUB-1478
September 1974
(T/E)

$e^+e^- \to$ HADRONS*†

B. Richter

Stanford Linear Accelerator Center
Stanford University, Stanford, California 94305

*Plenary Session Report at XVII International Conference on High Energy Physics, London, July 1974

†Work supported by the Atomic Energy Commission

1. INTRODUCTION

I will review the subject of hadron production in electron-positron collisions. The subject is of great intrinsic interest because of what it has to tell us about hadron structure and dynamics. The results of hadron production experiments in e^+e^- collisions should be relatively simple to understand because the process should proceed through one photon annihilation (Fig. 1a), in which the electron and positron annihilate to form a massive photon with J^{pc} of 1^{--} and precisely defined S (square of the center-of-mass energy). This is a particularly simple laboratory in which to test our understanding of hadron physics. For example, in the sample quark-parton model,hadron production proceeds as is shown in Fig. 1b and the cross section is calculated to be proportional to e^2 (from the photon electron vertex) x $\frac{1}{S}$ (from the photon propagator) x the sum of the squares of the quark charges (the sum of the contributions from each quark type). The energy dependence of this cross section is simply $\frac{1}{S}$ and the magnitude depends only on the type of quark model. In contrast to the simplicity of electron-positron annihilation, the situation is very much more complicated in hadron-hadron collisions, where the angular momentum, parity and charge conjugation quantum numbers are all unknown, and where, in the constituent models, not even center-of-mass energy is known.

This subject is of particular interest at the present time because the results of recent experiments flatly contradict all models of hadron production available up to about half a year ago. The results of these experiments were expected to be of a certain simple form on the basis of an elementary quark-parton model, which model has been, and is still very good at explaining many features of hadron decays, multiplet structures, scaling in inelastic electron scattering and some cross section relations. As we will see, the measured cross sections don't look at all like what was expected and one result is that there have been 66 contributions to this conference session - five experimental and sixty-one theoretical.

II. QUANTUM ELECTRODYNAMICS

I will begin with a review of the new experimental results on the validity of quantum electrodynamics. These experiments are important because quantum electrodynamics is our only successful field theory and is a model for many other theories, and because the validity of quantum electrodynamics is essential if our assumption that the initial state of hadron production in e^+e^- collisions is well understood is to be true. Figure 2 shows the Feynman diagrams for three electrodynamic processes for which new data is available. Bhabha scattering (Fig. 2a) involves both space-like and time-like photon exchange with the contribution from space-like exchange dominant (applitudes for space-like and time-like photon exchange are equal at 180°). Muon pair production is shown in Fig. 2b and involves time-like photon exchange and also allows checks to be made on muon-electron universality. The two photon annihilation process is shown in Fig. 2c and allows studies of off-the-mass-shell (space-like) leptons.

Two of these experimental contributions come from experiments done at the SLAC electron-positron storage ring SPEAR and the third comes from analysis of results from the CEA bypass project. Beron[1] et al. (SPEAR) used large sodium iodide crystals and spark chambers to study Bhabha scattering, μ-pair production, and two photon annihilation. Measurements were made at a center-of-mass energy of 5.2 GeV and at an angle of 90°. The normalization was made to Bhabha scattering at 3.7°. Approximately 500 Bhabha events, 80 mu-pair events and 88 2-photon annihilations were accumulated. The SLAC-LBL Magnetic Detector group [(2)] (SPEAR) used their large solid angle solenoidal magnetic spectrometer to measure Bhabha scattering and mu-pair production. The data cover an angular range from approximately 50° to 130°, and the experimental limits on quantum electrodynamics come from fits to the angular distribution of Bhabha scattering and mu-pair production. Data were taken at center-of-mass energies of 3, 3.8 and 4.8 GeV and, at the highest energy, 8000 Bhabha and 600 mu-pair events were accumulated.

Law *et al.*[(3)] (CEA) used the Bold detector, which is a shower counter and spark chamber laminate, to investigate the 2-photon annihilation process. Measurements were made in the angular region from 53° to 127° and normalization was to double bremsstrahlung at 0°. Twenty-eight 2-photon annihilation events were accumulated.

Beron *et al.* and the SLAC-LBL group have used a common parameterization of a possible breakdown of quantum electrodynamics[(4-6)]. In this formulation a form factor is associated with the photon propagator and is given by

$$F_{\gamma}^{\pm}(q^2) = 1 \pm \frac{q^2}{q^2 - \Lambda_{\pm}^2(\gamma)} \approx 1 \mp \frac{q^2}{\Lambda_{\pm}^2(\gamma)} \qquad (1)$$

where the + or - sign refers to the positive or negative metric formulation, and q^2 is the 4-momentum transfer. For tests of μ-e universality these groups used a form factor of

$$F_L(q^2) = 1 \pm \frac{q^2}{q^2 - \Lambda_{\pm}^2(L)} \approx 1 \mp \frac{q^2}{\Lambda_{\pm}^2(L)} \qquad (2)$$

at the lepton vertex. For 2-photon annihilation, the form factor of

$$F_e^{\pm}(q^2) = 1 \pm \frac{q^4}{\Lambda_{\pm}^4(e)} \qquad (3)$$

is used to characterize the virtual lepton. Law et al. have used a slightly different parameterization for their paper and I have recast their results in the form given above so that an intercomparison can be made between all of these experiments. All of these experiments used the radiative correction formulation of Berends et al.(7,8) which is calculated to order α^3.

TABLE 1

95% Confidence Limits on Cutoff Parameters in QED

	Photon Propagator			
	Λ_+		Λ_-	
Beron et al.	23		14	
SLAC-LBL(1)	16		13	
SLAC-LBL(2)	35		33	
	Lepton Form Factors			
	$\Lambda_+(e)$	$\Lambda_+(\mu)$	$\Lambda_-(e)$	$\Lambda_-\mu$
Beron et al.	-	15	-	24
SLAC-LBL	24	14	19	16
	Electron Propagator			
	Λ_+		Λ_-	
Beron et al.	6.2		6.9	
Law et al.	5.0		5.3	

The results of these experiments are summarized in Table 1. All entries in the table correspond to 95% confidence level lower limits to the cutoff parameters. For the photon propagator Beron et al. find 23 and 14 GeV limits on Λ_+ and Λ_-, respectively. The SLAC-LBL group find 16 and 13 GeV limits for Λ_+ and Λ_- by one method of analysis where only scattering data is used and a fit is made to the angular distribution with the normalization allowed to vary to minimize Λ. In the other SLAC-LBL calculations both Bhabha and mu-pair data are used with the ratio of mu-pairs to Bhabha scattering fixed by quantum electrodynamics.

For mu-e universality, Beron et al. find 15 and 24 GeV limits for Λ_+ and Λ_- where the form factor of the electron is assumed equal to 1. The SLAC-LBL group find Λ of $\geq$20 GeV for the electron vertex form factor and $\gtrsim$15 GeV for the mu vertex form factor using both Bhabha and mu-pair data.

For the 2-photon annihilation process Beron et al. find a cutoff in the lepton propagator of $\geq$6.5 GeV while Law et al. find about 5.1 GeV.

In summary once again all experiments agree with predictions of quantum electrodynamics and the lower limits on cutoff parameters have now risen to approximately 20-30 GeV for the photon propagator, 20 GeV for electron and mu form factors and about 6 GeV for virtual leptons.

III. HADRON TOTAL CROSS SECTIONS

New data from Frascati, CEA, and SPEAR on the total cross section for hadron production in electron-positron collisions are available which cover the entire range of S from 1-25 GeV^2. The S region from 1.5 to 9 GeV^2 has new data from the BCF group(9); the region from 7 to 24 GeV^2

has new data from the SLAC-LBL magnetic detector group[2] and the final analysis of the CEA point at $S = 25\ GeV^2$ is also available.[10] The trigger for all these experiments requires ≥ 2 charged particles in the final state. To be included in the multihadron classification, if only two charged particles go into the apparatus,these particles must be acoplanar by an angle ranging from 10° to 20° depending on the experiment. The apparatus for all three experiments covers polar angles from approximately 45° to 135° but the azimuthal angular coverage differs. The BCF group has an acceptance of a third in azimuthal angle, CEA two-thirds and SLAC-LBL one. The resulting total solid angles for these three experiments are 20%, 50% and 70% of 4π, respectively.

Since none of these experiments cover the full 4π solid angle, a correction must be made to account for the uncovered parts of the apparatus. The smaller the trigger solid angle, the larger this correction will be. The BCF group uses an all pion isotropic phase space model fit to the observed charged particle multiplicities to obtain an efficiency (observed over expected events) which rises from approximately 1% at the low energy end of their experiment to about 2% at the high energy end. With a correction factor which ranges from 50-100 between the observed cross section and the calculated total cross section, the absolute values of σ_{TOT} seem to me to be somewhat uncertain. While the relative cross sections between neighboring energy points should be quite good there may be large systematic errors from one end of the energy region to the other. (Low efficiency is something of a problem with all previous Frascati total cross section measurements, and probably accounts for the different experiments obtaining cross sections which differ by amounts larger than the stated errors).

The efficiency problem is much less severe for CEA and the SLAC-LBL group. CEA also uses an all pion isotropic phase space model to obtain an efficiency of 43% at S = 25. The SLAC-LBL magnetic detector group use 3 different models - the first being an all pion isotropic phase space model; the second being an isotropic phase space model which includes etas, K mesons, nucleons and antinucleons; and the third being a pure jet model with the jet axis distributed as $1 + \cos^2\theta$ and a jet decay with bounded transverse momentum. These 3 very different models give efficiencies which vary by $\pm 5\%$ and this uncertainty is included in the total of $\pm 10\%$ systematic errors on data points. The efficiency for the SLAC-LBL experiment ranges from 45% at S = 7 to 65% at S = 24.

The total cross section data is shown in Fig. 3. The measured total cross section falls rapidly as S increases from 1.5 to 8 or 9, and then appears to flatten out. The cross section ranges from about 25 nb at S = 8 to about 20 nb at S = 25 and is not at all consistent with an S^{-1} energy dependence in this region.

Figure 4 shows the ratio (R) of the total hadronic cross section to mu-pair production. The previously published points from the Frascati $\mu\pi$ and $\gamma\gamma$ groups and the Novosibirsk points[(11)] are included. The large spread in the values of the R at low energy reflects the detection efficiency problem mentioned earlier. In the region below S = 9, R seems to lie between 2 and 3 and rises smoothly to about 6 at S = 25. These results are in violent disagreement with the predictions of the simple quark model which range from 2/3 for the simple 3-quark model to 4 for the Han-Nambu model. A large fraction of the theoretical contributions to the conference attempt to explain this peculiar variation of R.

The approximate constancy of the total cross section with energy has generated sufficient surprise to prompt many people to ask whether or not these high energy events are indeed from one photon annihilation. It is not possible to answer the question unambiguously but we can eliminate three possible explanations - background, photon-photon collisions, and heavy lepton production. The background in all these experiments was measured by separated beam runs and found to be small - approximately 3% to 5% in the CEA and SLAC-LBL experiments and 10% to 15% in the BCF experiments. These backgrounds have been subtracted from the results.

The photon-photon process is illustrated schematically in Fig. 5. Both the incoming electron and positron radiate almost real photons which in turn react to produce the hadrons. These reactions are characterized by the presence of electrons and positrons at small angles to the beam direction in the final state as well as by the presence of hadrons. The cross section is roughly given by

$$\sigma \propto \frac{\alpha^4}{M_h^2} \left(\ln \frac{E}{m_e}\right)^2 \qquad (4)$$

where M_h is the mass of the produced hadron system. This cross section can become comparable with the one photon annihilation cross section in spite of the extra α^2, for the denominator contains M_h^2 instead of S and the numerator contains a $\log^2 \frac{E}{m_e}$. The ratio of this cross section to the mu-pair production cross section is given by

$$\frac{\sigma_{\gamma\gamma}}{\sigma_{\mu\mu}} \propto \alpha^2 \left(\ln \frac{E}{m_e}\right)^2 \frac{S}{M_h^2} \qquad (5)$$

and is expected to be small when the sum of the hadron energy is not small. For example, Brodsky has estimated the total cross section for this process will be less than one nanobarn when the total energy of the hadron system is greater than 1 GeV.[12]

Previous attempts to measure the contribution of this photo-photon collision process to the observed hadron production cross section have given upper limits to the contribution on the order of 10%. The SLAC-LBL group has measured this process with a small angle tagging system which is illustrated schematically in Fig. 6. Four small shower counters are interrogated whenever the main apparatus triggers. They have looked for the following reactions:

$$e^+ + e^- \rightarrow e^+ + e^- + e^+ + e^- \qquad (6a)$$

$$e^+ + e^- \rightarrow e^+ + e^- + \mu^+ + \mu^- \qquad (6b)$$

$$e^+ + e^- \rightarrow e^+ + e^- + \text{hadrons} \qquad (6c)$$

The group looks for events where there is a pulse in one of the tagging counters coincident with other particles in the final state. The tagging efficiency for single tags with this apparatus lies somewhere between 3% and 5%. The data is still under analysis but one can say that reactions (6a) and (6b) are both seen at a rate which is within a factor of 2 of the predicted rate, which proves that the apparatus does function as it is supposed to. In reaction (6c), no events are seen that are not consistent with the chance coincidence rate and this leads to a 95% confidence upper limit that less than 10% of the multi-hadron cross section can come from the photon-photon process.

Two limits on heavy lepton production have been reported - one by

Feller et al.[13] based on the CEA 5-GeV data, and one by Perl using the SLAC-LBL 4.8 GeV data. The experimenters search for electron, muon and hadronic decay modes. The usual heavy lepton decay branching ratios calculated assuming R=2 are

Mode	Branching Ratio
$e + \bar{\nu}_e + \nu_\ell$	0.2
$\mu + \bar{\nu}_\mu + \nu_\ell$	0.2
$\pi + \nu_\ell$	0.08
2 hadrons + ν_ℓ	0.52 .

Since R is around 2 at the upper limit of lepton mass allowable in these experiments, these are reasonable numbers to use.

Feller et al. used somewhat different branching rations and I have recomputed their results using the above numbers. They find 3 events with 3 background events expected for a net signal of 0 ± 2.4 events. The production of a heavy lepton pair gives an expected signal of 2.8 events.

The SLAC-LBL group find 35 events with 40 background events expected for a net signal of -5 ± 9. The expected signal from a heavy lepton pair is 40 events.

In summary, there seems to be no evidence for a heavy lepton with a mass less than about 2 GeV.

V. INCLUSIVE DISTRIBUTIONS

The SLAC-LBL group is the first to use a magnetic field to measure the momentum of the hadrons in the final state and hence to allow a determination of the inclusive momentum distributions. Before discussing the data it is useful to write down what one might expect for this inclusive distribution. Eq. (7) shows the general form of the differential cross section.

$$\frac{d^2\sigma}{dEd\cos\theta} = \frac{4\pi\alpha^2}{S} Mp \left(2W_1 + \frac{E\beta^2}{MS^{\frac{1}{2}}} \nu W_2 \sin^2\theta\right) \tag{7}$$

where p, E, β, and M are the momentum, energy, velocity and mass of the hadron, W_1 and W_2 are the structure functions which can in general be functions of both E and S; ν is defined by

$$M\nu = p.q \quad \text{(4 vector product).} \tag{8}$$

Defining a new variable x as

$$x = 2p.q/q^2 \tag{9}$$

the equation can be rewritten as

$$\frac{d\sigma}{dx} = \frac{4\pi\alpha^2}{S} \beta x (2MW_1 + \frac{\beta^2 x}{3} \nu W_2). \tag{10}$$

The Bjorken scaling hypothesis which works so well for inelastic electron scattering and neutrino reactions implies that the structure functions W_1 and νW_2 are functions of x along, and that therefore to within factors of β

$$S \frac{d\sigma}{dx} = f(x). \tag{11}$$

We know already that Equation (11) must be in error, for the integral of the left hand side of the Equation (11) is just equal to the mean particle multiplicity times the ratio of total hadronic cross section to mu-pair production. We have seen (Fig. 4) that this ratio is increasing and we will see later that mean multiplicity is also increasing.

Figure 7 shows the SLAC-LBL data for $S \frac{d\sigma}{dx}$ vs x at the three center of mass energies of 3, 3.8 and 4.8 GeV. The graph shows that scaling is not good for $x < \frac{1}{2}$, and that scaling appears to be good for $x > \frac{1}{2}$. Figure 8 shows the same data plot on a log scale, where we can see how good scaling is in the region above $x = 1/2$. Scaling appears to be good for $x > \frac{1}{2}$ at a level of around 10%.

There does seem to be a kind of scaling at low momentum. Figure 9 shows a plot of the differential cross section per unit Lorentz invariant phase space versus momentum. All three energies now superpose for momenta less than 1 GeV/c in what might be called "hadronic scaling". The solid lines on Fig. 9 are the data of Cronin et al.[14] on π production at 90° C.M. in p-p collisions at 200 GeV. This data is plotted vs. $p_\perp$ and has been renormalized to show the similarity in the slopes of the inclusive cross sections for pions produced in the two reactions. The e^+e^- data breaks away from the p-p data at the momentum where Bjorken scaling begins to hold.

Figure 10 shows the mean charged particle multiplicity as measured at Frascati,[15] CEA[13] and SPEAR,[2] together with the charge multiplicity measured in several $\bar{p}p$ annihilation experiments.[16] The mean charged particle multiplicity in e^+e^- collisions is a very slowly varying function ranging from 3.8 at 3 GeV in the center of mass to 4.2 at 5 GeV in the center of mass and seems to vary less rapidly than log S.

Figure 11 shows the SLAC-LBL data on the mean charged particle momentum. This also is a very slowly varying function going from about 430 MeV at 3 GeV in the center of mass to 520 MeV at 4.8 GeV in the center of mass. This distribution also seems to vary less rapidly than log S.

Figure 12 shows the total energy in charged particles divided by the total energy in hadrons vs. center-of-mass energy. There is data from both the SLAC-LBL group and the Frascati $\gamma\gamma$ group.(16) All particles are assumed to have the pion mass and the denominator excludes the approximately 3% to 5% of the incident energy calculated by the standard radiative correction formula to be radiated as hard gamma rays along the beam direction. This ratio changes from about 63% at 3 GeV in the center of mass to around 50% at 4.8 GeV in the center of mass. This decrease in the ratio of charged particles energy to total energy is what has been referred to as "the energy crisis". There is a problem only in those models which insist on producing only pions in the isospin 0 state.

VI. ANGULAR DISTRIBUTION

In one photon annihilation the angular distribution of any particle is forced by angular momentum conservation to be of the form

$$\frac{d\sigma}{d\cos\theta} \propto 1 + \alpha\cos^2\theta \qquad (12)$$

where the coefficient of $\cos^2\theta$ must lie between ± 1. Different models can give different values for the parameter α but angular momentum conservation determines the upper and lower bounds. For example, parton models using spin 1/2 partons have $\alpha = +1$ while a spin zero point particle model gives $\alpha = -1$. In the simple quark model, quarks somehow decay to hadrons and this decay process can wash out the features in the angular distribution for low-momentum final-state hadrons, but in the limit of

$x \to 1$ the coefficient alpha must also go to 1.

Table 2 gives the results of the SLAC-LBL experiment for α.

Table 2

Values of α in the $1 + \alpha \cos^2\theta$ fit to the

Angular Distribution

$\sqrt{s}$	α	
	x 0.45	0.45 x 0.9
4.8	0.25 ± 0.10	0.2 ± 0.2
3.8	0.18 ± 0.11	0.0 ± 0.4
3.0	0.0 ± 0.17	0.2 ± 0.4

Data are presented for 3 energies and 2 regions of x. α is small at all of these points which is a challenge to model builders. The SLAC-LBL group has also looked for jet structure in their data. They search for jets by defining a quantity called "sphericity" as follows.

For each event compute:

(1) $T_{\alpha\beta} = \Sigma \left({}_{\alpha\beta}P_i^2 - P^i_{\alpha} P^i_{\beta} \right)$

(2) Diagonalize $T_{\alpha\beta}$; $\lambda_i = \Sigma P^2_{\perp_i}$

(3) Define Sphericity (SP) as

$$SP = \frac{3\lambda_3}{\lambda_1 + \lambda_2 + \lambda_3}$$

The sphericity is zero for an event with colinear particles (mu-pair production for example). Unfortunately this test is not sensitive at present energies. Table 3 shows a comparison of the sphericity for an isotropic invariant phase space model compared to a pure jet model with bounded transverse momentum (both models are adjusted to fit the mean multiplicity and mean energy in charged particles). Only a 20% effect

Table 3

Comparison of Sphericity in an Isotropic Phase Space Model and a Jet Model

$\sqrt{S}$ (GeV)	Sphericity	
	1 PS	JET
5	0.33	0.26
8	0.34	0.17
30	0.39	0.04

is possible at present energies but the sensitivity of this test improves markedly as the center-of-mass energy increases. Present results give a value for the sphericity about 10% below the invariant phase space models and are inconclusive. Meaningful tests for jets will have to wait for higher energies at SPEAR and at DESY.

VII. HEAVY PARTICLE PRODUCTION

Preliminary results on K meson and antiproton production are available from the SLAC-LBL group. Figure 13 shows the measured number of π^-, K^- and $\bar{p}$ at the center-of-mass energy of 4.8 GeV. Particles are identified by a time-of-flight system referenced to the time of collision of the short bunches of electron and positrons circulating in the SPEAR storage ring. This system can resolve K mesons (3σ) at a momentum of up to 600 to 700 MeV/c and antiprotons up to 1 to 1.2 GeV/c. The π^- yield (Fig. 13) is seen to fall, the K^- yield seems to be going up, and the antiproton yield is flat. The protons are not analyzed in this experiment because of a problem with background coming from residual gas interactions. While these beam-gas events amount to only 3% to 5% of the total number of hadronic events, they preferentially have protons in them. In fact, the measured proton yield is twice the antiproton yield. There is no contamination in antiprotons because the energy of the beams is below threshold for antiproton production in an interaction with a nucleus at rest.

Figure 14 shows the 4.8 GeV data plotted as the fraction of a given particle type, versus momentum. The pions are seen to be falling, the K's to be rising and the antiprotons to be rising. The K/π ratio at the maximum momentum where separation is possible has risen to about one fourth. The data at 3.8 and 3 GeV are similar (the errors are bigger and there are not enough antiprotons at the lower energy to be statistically significant).

The Princeton-Maryland-Pavia collaboration (at SPEAR) has reported at this meeting(17) a preliminary measurement of the K/π ratio integrated over all momenta ≤ 1 GeV/c. They find that $K/\pi = 0.4 \pm 0.2$.

Figure 15 shows data from the ISR(18) and NAL(19) on heavy particle production. This data is remarkably similar to that seen in the e^+e^- collisions in the region where the data points overlap.

Figure 16 shows the negative particle yield per unit invariant phase space versus the total energy of the particle. I don't really know what this graph means but it is remarkable that all the points seem to fall on one line corresponding to a temperature of 164 MeV. We know this cannot continue to high momenta, for at high momenta the inclusive distribution breaks away from an exponentially falling distribution (see Fig. 9). In the low energy region however, one line seems universal and it appears that the yields don't particularly care about quantum numbers such as Baryon number, strangeness or spin, but only depends on the total energy.

VIII. EXCLUSIVE CHANNELS

The only new data on exclusive channels presented at this Conference is from the SLAC-LBL group on the reactions

$$e^+ + e^- \rightarrow 2\pi^+ + 2\pi^- \quad (13a)$$

$$e^+ + e^- \rightarrow 3\pi^+ + 3\pi^- . \quad (13b)$$

Reaction 13a is isolated from the data by kinematic fitting to those events which have four charged particles observed (4 constraints) and to those events with three charged particles observed (one constraint), while reaction 13b is isolated by similar fits to 6 and 5 observed charged particles. New data for the four charged-particle final-state is shown in Fig. 17 together with previous Frascati data.[20] The curves are phase-space calculations by Schwitters.[21] The new data drops smoothly at high energy to a low value of approximately 0.1 nb at 4.8 GeV. (We look forward to new data from the Frascati magnetic detector group which will allow us better to pin down the properties of the ρ''.) Figures 18a and 18b show the invariant mass distribution for charge zero and charge 2 pairs. The dotted lines on these curves show the expected phase space distribution normalized to the total number of events. No compelling evidence either for or against the production of ρ or f mesons is to be seen.

Figure 19 shows the cross section for the six charged pion channel from SLAC-LBL and Frascati.[22] The curve is again Schwitter's phase space model. The data once more falls smoothly to about the 0.1 nb level. The shape and magnitude of the cross section is similar to that for the 4-charge pion state above 3 GeV in the center of mass. The mass distribution for charge 0 and charge 2 pairs from the 6 pion data is shown in Figs. 20a and 20b. Again there is no compelling evidence for or against meson resonance production.

IX. EXPERIMENTAL SUMMARY

The experimental data can be summarized briefly as follows:

(1) Quantum electrodynamics has triumphed again. The 95% confidence lower limit on a cut-off momentum is about 30 GeV for the photon propagator, 20 GeV for μ-e universality, and about 6 to 7 GeV for a virtual electron.

(2) The total hadronic cross section falls rapidly with S until an S of 8 or 9 GeV^2 is reached, and flattens out to lie between 20 to 25 nb from S of about 9 to S of about 25 GeV^2. It could be very slowly falling.

(3) The ratio of the total hadronic cross section to μ-pair production rises from a value of about 2.5 at S=9 and reaches about 6 at S=25.

(4) The mean charged particle momentum and the mean charged particle multiplicity both rise very slowly with energy.

(5) Inclusive distributions show Bjorken scaling above x = 1/2 and hadronic scaling below $x = \frac{1}{2}$. The slope of the differential cross section per unit invariant phase space agrees well with that observed for pion production in p-p reactions.

(6) The angular distribution is very roughly isotropic for both low and high x.

(7) The ratios of K meson to pi-meson production and antiproton to pi-meson production increase with increasing momentum at fixed S. The K to pi ratio is not strongly dependent on S.

(8) Four and six charged particle exclusive cross sections fall smoothly with S and at S = 24 are each equal to about 0.1 nb, i.e., 0.5% of the total cross section.

All of the above coupled with the deep inelastic electron scattering results, the deep inelastic muon scattering results from NAL, and the inelastic neutrino reaction results is going to make quite a difficult collection of data for the theorist to explain.

X. THEORY

The e^+e^- annihilation data contradict both the simple quark-parton model and the Bjorken scaling hypothesis. This has come as a shock for they were both doing so well - giving an understanding of multiplet structure, cross section relationships, decay branching ratios, deep inelastic electron, neutrino, and muon scattering, etc. Indeed, scaling was tested and found to work to 10% to 20% over three orders of magnitude in the structure functions and for values of momentum transfer ranging up to 60 to 70 $(\mathrm{GeV}/c)^2$ and values of inelasticity out to 100 GeV. Most of the 61 theoretical contributions to this session of the Conference, which range from the bizarre to the ordinary, attempt to resolve the contradiction between the success of simple models in the space-like momentum transfer region and their failure in the time-like momentum transfer region.

I am supposed to review these contributions for you. I clearly cannot review them all for time is short and I do not understand half of them. (These papers have been reviewed by Ellis and Renard in the parallel session and their reviews are included in the Conference proceedings.) I will instead select a few examples of different kinds of models, try to describe their assumptions and predictions, and test them against the data where possible. I will begin with my favorite - models involving new lepton-hadron interactions.

A. New Interactions

When I first saw our data in the SLAC-LBL experiment I was struck by the similarity of certain features such as the roughly constant cross section, the slope of $Ed\sigma/d^3p$ at low momentum, heavy particle yields, and mean multiplicities to similar features seen in hadronic interactions. I suggested then that perhaps electrons had strong interactions of very short range and that what we were seeing was not 1 photon annihilation but a kind of no-photon annihilation. I soon discovered I had some very distinguished company for Pati and Salam had been working on such a scheme for some time. Others began working along these lines and at this Conference we have contributions from Pati and Salam(23), Greenberg and Yodh(24), Nanopolous and Vlassopoulos(25), and Budini and Furlan(26). I will describe two of these models.

Figure 21a shows the quark scheme of Pati and Salam which unifies the leptons with a standard set of quarks with color and charm in a kind of Han-Nambu scheme. The model comes with a set of gauge bosons which couple the leptons to the quarks, and hadron production in e^+e^- interactions proceeds by the exchange of one of these bosons as shown in Figure 21b. Working through the model as originally formulated, they find that their gauge bosons are too heavy to account for the cross section. On the reasonable assumption that no one knows how to calculate the mass of gauge particles, Pati and Salam apply their model to e^+e^- reactions and to deep inelastic lepton scattering.

In the model, the cross section for hadron production has the form -

$$\sigma(e^+e^- \rightarrow \text{hadrons}) = \frac{C_1}{S} + C_2 + C_3 S \qquad (14)$$

where the S^{-1} term represents the one photon annihilation, the S term is due to the new interaction, and the constant term is an interference which depends on the form of the direct coupling. In Figure 3 the cross section below S=9 is dominated by the one photon term, while between S=9 and S=25 the interference term dominates. The model makes the spectacular prediction that at higher energy the cross section must increase.

For inelastic lepton scattering, the model allows a difference between positive and negative lepton cross sections (depending on the choice of coupling) and also predicts a violation of scaling. Taylor in one of the parallel sessions[27] reported an experiment measuring the ratio of e^+ to e^- inelastic scattering up to a maximum q^2 of 15 $(\text{GeV}/c)^2$. His group found the ratio to be 1 ± 0.1 before radiative corrections. Scaling is also known to be good at SLAC energies up to q^2 of about 20 $(\text{GeV}/c)^2$.

The Pati-Salam model is marginally consistent with these experiments, but to be consistent with hadron production in e^+e^- collisions, scaling must break down at higher q^2. Note however that since the muon is coupled to strange quarks, the effect may not be seen in the NAL muon experiments. The critical test of this model is the predicted increase in the e^+e^- cross section at energies soon to be available at SLAC and DESY.

A quite different approach has been taken by Greenberg and Yodh. They use the Mueller graph shown in Figure 22. (If you don't already understand Mueller graphs, I can't help you.) This process is diffractive and leads to typical strong interaction distributions. The cross section is given by

$$E \frac{d\sigma}{d^3p} = A \exp\left(-ap_\perp - b X_{11}^2\right) \qquad (15)$$

where $p_\perp = p \sin\theta$ and $X_{11} = 2p\cos\theta / S^{\frac{1}{2}}$. The inclusive distribution shows the correct shpae at low momentum, but does not show scaling at $x > \frac{1}{2}$.

A more serious problem occurs in the angular distribution. The Greenberg-Yodh angular distribution is indeed quite flat in the region measured in experiments to date, when integrated over all momenta. However, it is anything but flat for a momentum greater than a few hundred MeV/c. Figure 23 shows the Greenberg-Yodh angular distribution for various momenta normalized to 1 at 90°. Also shown is the $1 + \cos^2\theta$ distribution to which the SLAC-LBL data was fit. The data shown in Table 2 would appear to exclude this model.

There are several papers on limits to possible direct interactions which can be derived from other experiments. Davies, Guy and Zia[28] find that the present limit on $\pi^0 \rightarrow e^+e^-$ appears to exclude a pseudoscalar coupling.

Bigi and Bjorken[29] with an effective Lagrangian which belongs to an SU_3 octet also exclude pseudoscalar coupling and find that other couplings give a breakdown of scaling in inelastic lepton scattering although higher q^2 will be required to show this effect. They, together with Goldman and Vinciarelli,[30] point out that all couplings except vector and axial vector give a cross section which depends on the polarization of the e^+ and e^- beams. Since the circulating beams in electron storage rings may become polarized, this effect may be a powerful one for looking for new kinds of interactions. Such measurements may be possible when SPEAR and DESY rings can run at energies of around 4 GeV where the polarization time is reasonably short. Beg and Feinberg[31] find a restrictive limit on axial vector interactions from the hyperfine structure splitting in hydrogen!

B. Patches and Fixes to the Quark Model

There have been 10 to 15 papers submitted which attempt to repair the simple quark model. Their common theme is "we should have known better". I will describe two of these.

West[32] and Chanowitz and Drell[33] suggest quark structure to account for the increase in the ratio of hadron to μ-pair production (R). West has worked out more experimental consequences and so I will concentrate on his work. The basic idea is that since quarks have strong interactions they must also have a finite size characterized by the mass of the gluon which couples the quarks. This generates a form factor of the form

$$F = \left(1 - \frac{q^2}{\Lambda^2}\right)^{-1} \approx 1 + \frac{q^2}{\Lambda^2} + \ldots \qquad (16)$$

which in turn makes R in the quark model equal to

$$R = \left(1 + \frac{q^2}{\Lambda^2}\right) \Sigma\, q_i^{\,2} \qquad (17)$$

where $\Sigma q_i^{\,2}$ is the usual sum of the squares of the quark charges. While this can fix the problem for e^+e^- annihilation, it generates serious violations of scaling in inelastic scattering. West adds an anomalous magnetic moment to the quark also generated by the strong interactions. Then for e^+e^- annihilation

$$R(e^+e^-) = \left[1 + \left(\tfrac{1}{2}\mu_q^2 + \frac{2}{\Lambda^2}\right)S\right] \sum_i q_i^2 \qquad (18)$$

while for inelastic lepton scattering

$$\nu W_2 = \left[1 - \left(\tfrac{1}{2}\mu_q^2 - \frac{2}{\Lambda^2}\right)q^2\right] \Sigma\, q_i^2 \quad . \qquad (19)$$

The two effects add in e^+e^- annihilation and cancel in inelastic scattering. This model can fit the cross section and requires R to increase to a maximum at E_{cm} = 8 to 10 GeV and then decrease.

Since West only adjusts the photon quark vertex to enhance $q\bar{q}$ production, Bjorken scaling should result if this enhancement is removed, i.e.,

$$\frac{1}{\sigma_{TOT}} \frac{d\sigma}{dx} = f(x) \ . \qquad (20)$$

Figure 24 shows this function plotted from the SLAC-LBL data. There is no scaling at any region of x. The conclusion which can be drawn from Figure 24 is that any model which modifies the photon-quark vertex, modifies the photon propagator, or adds more quarks but has free quarks produced, will not work. Quarks may be asymptotically free, but they are slaves now.

A very different model is that of Cheng and Mandula[34] which says that quarks are not only slaves now, but will always be so. They sum all higher order graphs shown in Figure 25 and find that each new order adds $\frac{1}{n!}(\ln S)^n$ to the amplitude. This results in a value of R given by

$$R = S^a\, \Sigma\, q_i^2 \qquad (21)$$

where the term S^a comes from summing the higher order terms. This model predicts in addition to Eq.(21),

$$\langle n \text{ charged} \rangle = \beta \ln s \tag{22a}$$

$$\frac{1}{\sigma_{TOT}} \frac{d\sigma}{dp} = f(p) \quad \text{for small } p \tag{22b}$$

$$\frac{1}{\sigma_{TOT}} \frac{d\sigma}{dx} = g(x) \quad \text{for } x \to 1 \ . \tag{22c}$$

These predictions are not violently in disagreement with the data, but the authors have not yet calculated what happens in inelastic lepton scattering.

C. <u>Hydrodynamic, Thermodynamic and Phase Space Models</u>

All these models share the following characteristics.

(1) None have anything to say about the cross section.

(2) All have a problem with $\langle n_{charged} \rangle$ <u>vs.</u> $\langle p_{charged} \rangle$. If $\langle n \rangle$ varies slowly, $\langle p \rangle$ varies rapidly and vice-versa.

(3) All give $d\sigma/dp$ which resembles the data at low momentum.

(4) All fail to show the Bjorken scaling seen in the data for $x > \frac{1}{2}$.

(5) All use pions only. The inclusion of η's, K's and P's might help with the $\langle n \rangle$ <u>vs.</u> $\langle p \rangle$ problem.

These models cannot illuminate the fundamental reaction process, nor can they describe those high momentum particles which are born "early" in the reaction, but they can be quite useful in calculating the production of lower momentum particles. Incidentally, no one seems to calculate the

the production of single photons. The temperature of the hot fluid or fireball is known to be about 170 MeV when it breaks up (see Fig. 16). An elementary calculation of black body radiation from an object with a temperature of 170 MeV, a radius of 10^{-13} cm and a lifetime of 10^{-13} cm/velocity of light indicates that the black body radiates 800 MeV in photons. This is certainly too simple minded a calculation, but can it have something to do with the energy crisis?

D. Resonance and Vector Dominance Models

Ferro-Fontan and Rubenstein(35) have a model using a photon-3 hadron coupling like that used in $\pi\,\Delta$ photoproduction. In this model a new channel opens whenever the photon energy equals the sum of the masses of any three resonances in the Rosenfeld tables. The coupling is full strength at threshold and is damped above threshold by an ad-hoc form factor so that the sum over all open channels yields a constant cross section. No calculations of multiplicity, neutral energy, heavy particle yield, or inclusive spectra have been made yet. It will probably be very difficult to fit all the data.

Terazawa(36) and Renard(37) have both used the vector dominance model to reach quite different conclusions. Terazawa has R reaching an asymptotic value of 6 to 7, while Renard's calculation using an infinite sequence of overlapping vector mesons indicates that R can increase for a while but must eventually drop to a lower value than it has at 25 $(\mathrm{GeV})^2$. Neither model makes any other prediction.

XI. CONCLUSIONS

Theory is in a confusing state and it is up to the experimenters to clear the air a bit. With the increase in energy of the SPEAR ring, the start up of the ring at DESY, and a new generation of apparatus at Frascati and Orsay, we can expect to see all of the results reported here extended to S_{max} of 70 to 80 $(GeV)^2$. In addition, experiments are in preparation to measure angular distributions down to 10° to 15°; π^0, η^0, K^0, Λ^0, and gamma-ray inclusive spectra; remeasure low energy data with large solid angle apparatus; and to extend limits on QED to values of Λ of about 50 GeV.

Hopefully, the resolution of the contradiction between lepton induced hadron production at time-like and space-like momentum transfer will lead to a new depth of understanding of the elementary particles.

References

1. B. L. Beron, J. F. Crawford, R. L. Ford, R. Hofstadter, E. B. Hughes, R. Kose, P. Le Coultre, T. W. Martin, L. H. O'Neill, R. E. Rand, L. Resvanis, R. F. Schilling, J. W. Simpson. Contribution 698 to this conference (HEPL 734 (1974)).

2. J.-E. Augustin, A. M. Boyarski, M. Breidenbach, F. Bulos, J. T. Dakin, G. J. Feldman, G. E. Fischer, D. Fryberger, G. Hanson, B. Jean-Marie, Rudolf R. Larsen, H. L. Lynch, D. Lyon, C. C. Morehouse, J. M. Paterson, M. Perl. T. Pun, B. Richter, R. F. Schwitters. (Stanford Linear Accelerator Center) G. S. Abrams, D. Briggs, W. Chinowsky, C. E. Friedberg, G. Goldhaber , R. J. Hollebeek, J. A. Kadyk, G. H. Trilling, J. S. Whitaker, J. E. Zipse. (Lawrence Berkeley Laboratory)

3. M. E. Law, J. Eshelman, J. Leong, A. Litke, R. Little, H. Newman, K. Strauch, G. Tarnopolsky, R. Wilson, Contribution 981 to this conference.

4. S. D. Drell; Annals of Phys. 4,75 (1958).

5. N. M. Kroll; Nuovo Cimento 45A,65 (1966).

6. T. D. Lee and G. C. Wick, Nucl. Phys. B9,209 (1969).

7. F. A. Berends, K. J. F. Gaemers, R. Gastmans; Nucl. Phys. B68, 541 (1974) and Nucl. Phys. B57, 381 (1973).

8. F. A. Berends, R. Gastmans; Nucl. Phys. B61, 414 (1973).

9. M. Bernardini, D. Bollini, P. L. Brunini, E. Fiorentino, T. Massam, L. Monari, F. Palmonari, F. Rimondi, A. Zichichi. Contribution 995 to this conference (to be published in Phys. Lett.).

10. G. Tarnopolsky, J. Eshelman, M. E. Law, J. Leong, H. Newman, R. Little, K. Strauch, R. Wilson; PRL 32, 432 (1974).

11. See review by K. Strauch in Proc. 6th Intl. Symposium on Electron and Photon Physics at High Energies pl. (H. Rollnick, W. Pfeil, eds. North Holland, 1974).

12. S. J. Brodsky in Proceedings of Intl. Colloquium on photon-photon collisions in electron-positron storage rings, Paris 1973. Journal de Physique, Colloque No. 2 Supp. No. 3, 1974.

13. J. Feller, A. Litke, J. Eshelman, J. Leong, H. Newman, G. Tarnopolsky, R. Wilson. Contribution 963 to this Conference.

14. J. W. Cronin, H. J. Frisch, M. J. Sochet, J. P. Boymond, P. A. Piroue, R. L. Summer; Phys. Rev. Lett. 31, 1426 (1973).

15. F. Felicetti, report in parallel session, this proceedings.

16. For multiplicities in $p\bar{p}$ annihilation see: T. Ferbel, A. Firestone, J. Sandweiss, H. D. Taft, M. Gailloud, T. W. Morris, W. J. Willis, A. N. Bachman, P. Baumel, R. M. Lee; Phys. Rev. 143, 1096 (1966): D. Everett, P. Grossman, P. Mason, H. Muirhead; Liverpool University Preprint, 1973: T. Ferbel, J. A. Johnson, H. L. Kraybill, J. Sandweiss, H. D. Taft; Phys. Rev. 173, 1307 (1968): J. Whitmore, private communication.

17. G. K. O'Neill, report in parallel session, this proceedings.

18. B. Alper, H. Bøggild, P. Booth, F. Bulos, L. J. Carroll, G. von Dardel, G. Damgaard, B. Duff, F. Heyman, J. N. Jackson, C. Jarlskog, L. Jonsson, A. Klovning, L. Leistam, E. Lillethun, G. Lynch, M. Prentice, D. Quarrie, J. M. Weiss; Phys. Lett. 47B, 275 (1973).

19. J. W. Cronin et al., Ref. 14.

20. F. Ceradini, M. Conversi, S. D'Angelo, L. Paoluzi, R. Santonico, K. Ekstrand, M. Grilli, E. Iarocci, P. Spillantini, V. Valente, R. Visentin, M. Nigro; Phys. Lett. 43B, 341 (1973); G. Barbarino, M. Grilli, E. Larocci, P. Spillantini, V. Valente, R. Visentin, F. Cerardini, M. Conversi, L. Paoluzi, R. Santonico, M. Nigro, L. Trasati, G. T. Zorn; Lett. Nuovo Cim. 3, 689 (1972).

21. R. Schwitters, SPEAR Report 178 (Stanford Linear Accelerator Center, 1974).

22. M. Grilli, E. Iarocci, P. Spillantini, V. Valente, R. Visentin, B. Borgia, F. Ceradini, M. Conversi, L. Paoluzi, R. Santonico, M. Nigro, L. Trasati, G. T. Zorn; Nuovo Cimento 13A, 593 (1973).

23. J. C. Pati, A. Salam, Contribution 79 to this conference.

24. O. W. Greenberg, G. B. Yodh, University of Maryland, Report 74-109. Contribution 547 to this conference.

25. D. V. Nanopoulos and S. D. P. Vlassopoulos, Report Number TH 1842-CERN (1974).

26. P. Budini, G. Furlan, Report Number IC/74/76 (ICTP, Trieste).

27. R. E. Taylor; report in parallel session on deep inelastic phenomena, this conference.

28. J. D. Davies, J. G. Guy, R. K. P. Zia. Report number RL-74-092 (Rutherford Laboratory) 1974.

29. I. I. Y. Bigi, J. D. Bjorken. Report number SLAC-PUB 1422 (Stanford Linear Accelerator Center) 1974.

30. T. Goldman, P. Vinciarelli. Report number SLAC-PUB 1407 (Stanford Linear Accelerator Center) 1974.

31. M. A. B. Beg, G. Feinberg. Report number COO-22328-52 (Rockefeller University) 1974.

32. G. B. West, P. Zerwas. Report Number SLAC-PUB 1420 (Stanford Linear Accelerator Center) 1974.

33. M. Chanowitz, S. D. Drell. PRL 30, 807 (1973).

34. H. Cheng. J. Mandula. Contribution 1022 to this conference.

35. C. Ferro-Fontan, H. R. Rubinstein. Report number TH 1810-CERN (1974).

36. H. Terezawa; Phys. Rev. Lett. 32, 694 (1974).

37. F. M. Renard: Contribution 24 to this conference.

Figure Captions

1. Feynman diagrams for hadron production in e^+e^- collisions: (a) general (b) simple quark model.
2. Feynman diagrams for (a) Bhabha scattering (b) muon pair production (c) 2-photon annihilation.
3. The total cross section vs. the square of the center-of-mass energy. Only data which became available in the last year is shown. The dashed curve is proportional to 1/S.
4. All measurements of the ratio of σ_{TOT} to $\sigma_{\mu\mu}$ vs. S, for $S \geq 1.5$ $(GeV)^2$.
5. Schematic of the two photon process.
6. Schematic of the SLAC-LBL tagging experiment.
7. The inclusive cross section vs. Bjorken scaling variable **x**.
8. Data of Figure 7 on a log scale.
9. The inclusive cross section per unit invariant phase space (left scale) vs. particle momentum. The lines are the data of Cronin et al, on π production at 90° C.M. in p-p collisions (right scale) vs. $p_\perp$. The solid lines are measured and the dashed lines at low $p_\perp$ are extrapolated.
10. Mean charged particle multiplicity vs. center of mass energy. Points from $p\bar{p}$ annihilation are included for comparison. The curve is log S normalized to fit the data at 3.5 GeV.
11. Mean charged particle momentum vs. $\sqrt{S}$ from the SLAC-LBL experiment. The curve is log S normalized to the data at around 3.5 GeV.
12. Total energy in charged particles divided by total hadron energy vs. $\sqrt{S}$.

13. Observed negative particle yields vs. momentum.

14. Negative particles as a fraction of all negative particles vs. momentum.

15. Same as 14 for p-p experiments.

16. Yield per unit invariant phase space vs. particle total energy.

17. Cross section for the exclusive 4-charged pion reaction vs. $\sqrt{S}$.

18. Invariant dipion mass distribution from the 4π states: (a) charge 0 pairs (b) charge 2 pairs. The dotted curves are phase space normalized to the same number of events as in the histograms.

19. Cross section for the exclusive 6-charged pion channel vs. $\sqrt{S}$.

20. Invariant dipion mass distribution from the 6π states: (a) charge 0 pairs (b) charge 2 pairs. The lines show the phase space distributions for the same number of events.

21. Pati-Salam model: (a) The quark scheme including leptons (b) Hadron production via the exchange of a gauge boson.

22. Mueller graph for the model of Greenberg and Yodh.

23. Angular distributions at various momenta from the model of Greenberg and Yodh. The dotted line shows the most rapidly varying distribution which can be obtained in one photon annihilation.

24. The inclusive distribution normalized to the total cross section vs. x. This should scale in West's model.

25. Feynman graphs for hadron production including higher order terms. Cheng and Mandula sum the infinite series of these graphs.

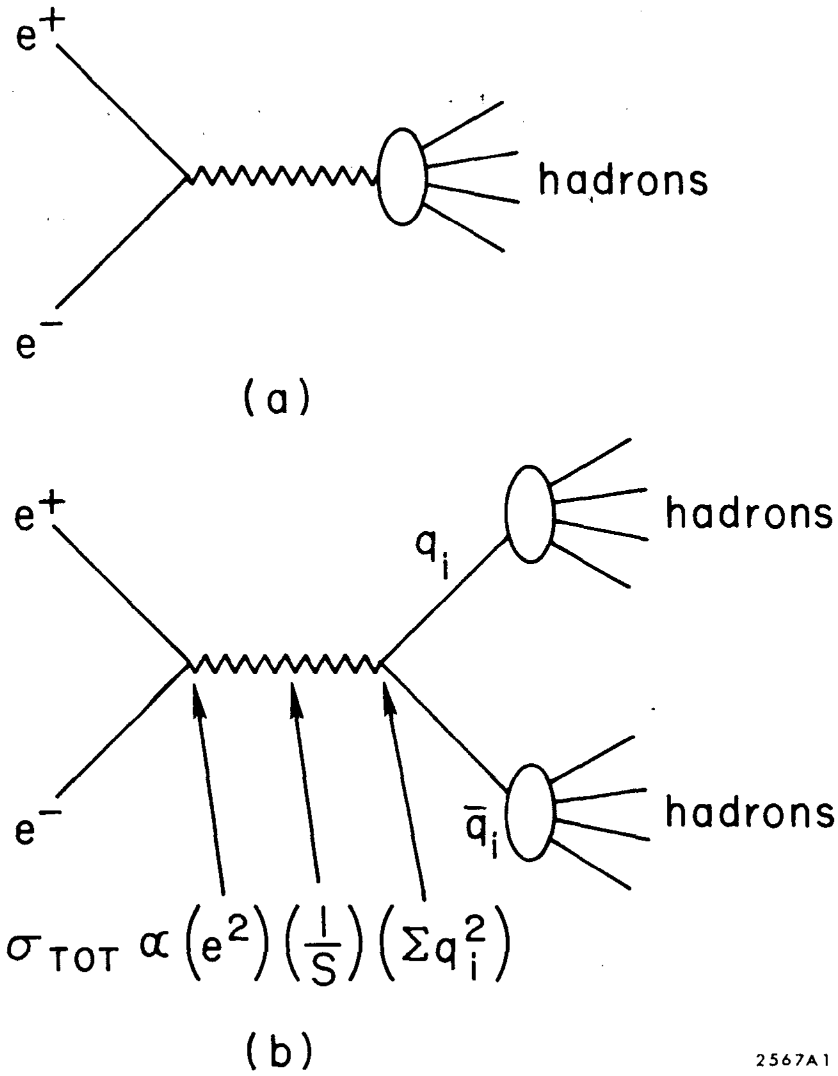
e+
e−
hadrons
(a)
e+
e−
q i
q̄ i
hadrons
hadrons
σ TOT α (e2) (1/S) (Σq i 2)
(b)
2567A1

Fig. 1

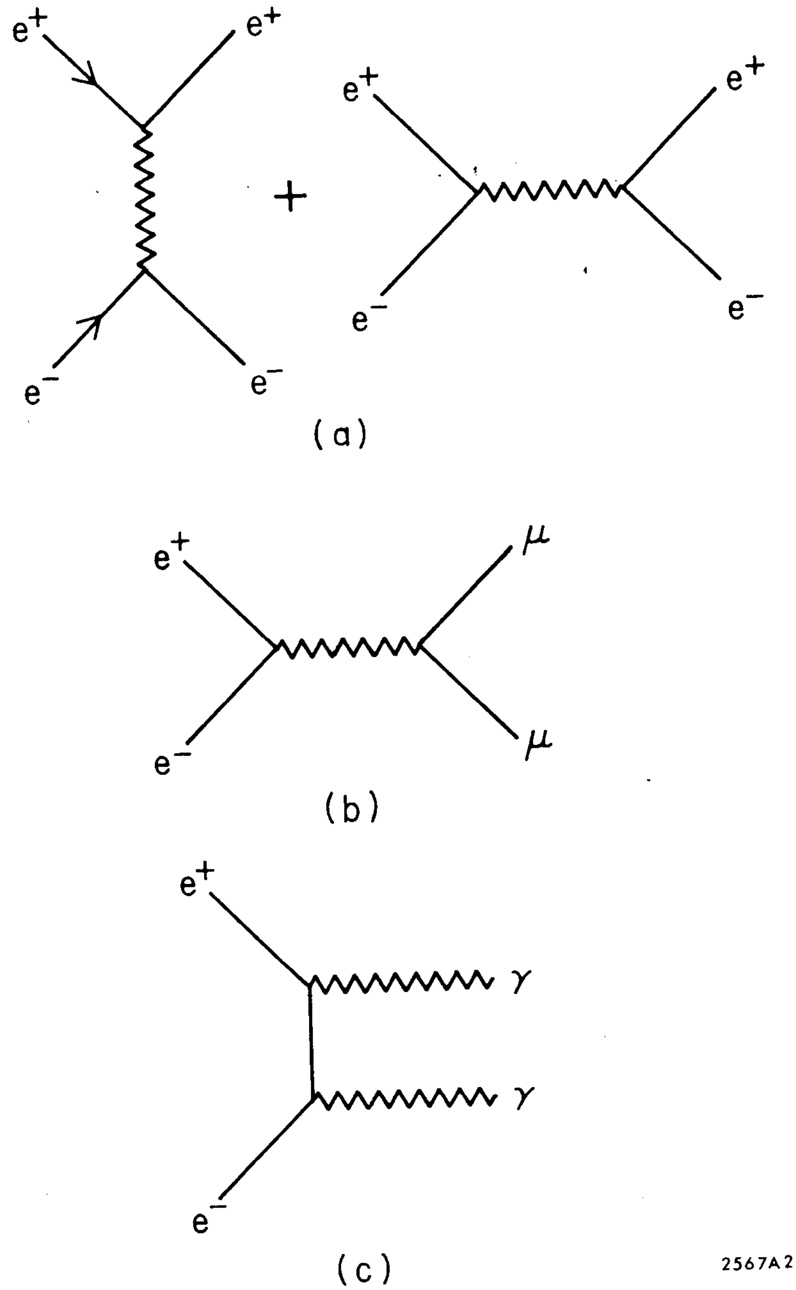

Fig. 2

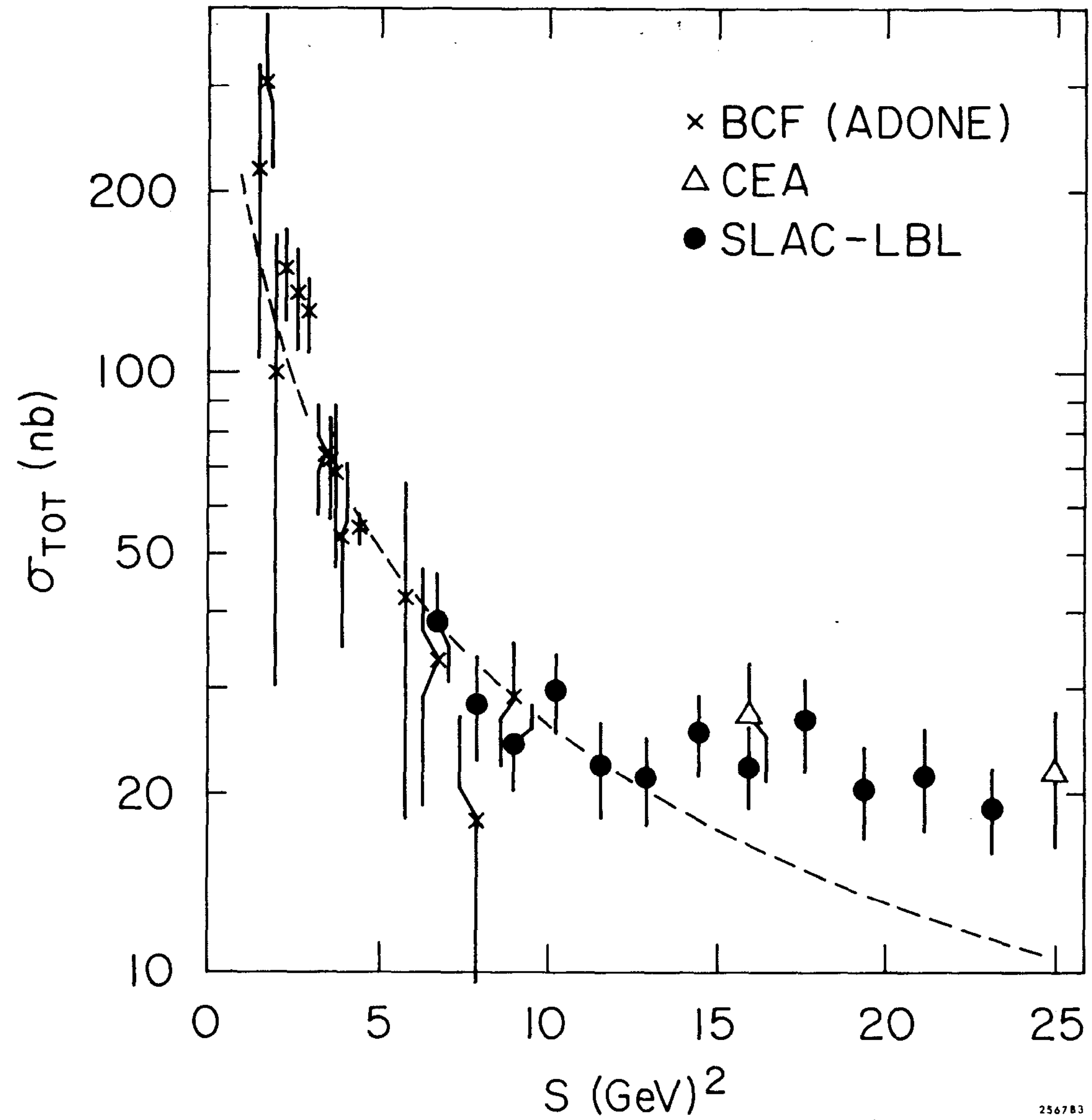

× BCF (ADONE)
△ CEA
● SLAC-LBL
200
100
50
20
10
σ_{TOT} (nb)
0
5
10
15
20
25
S (GeV)^2
2567B3

Fig. 3

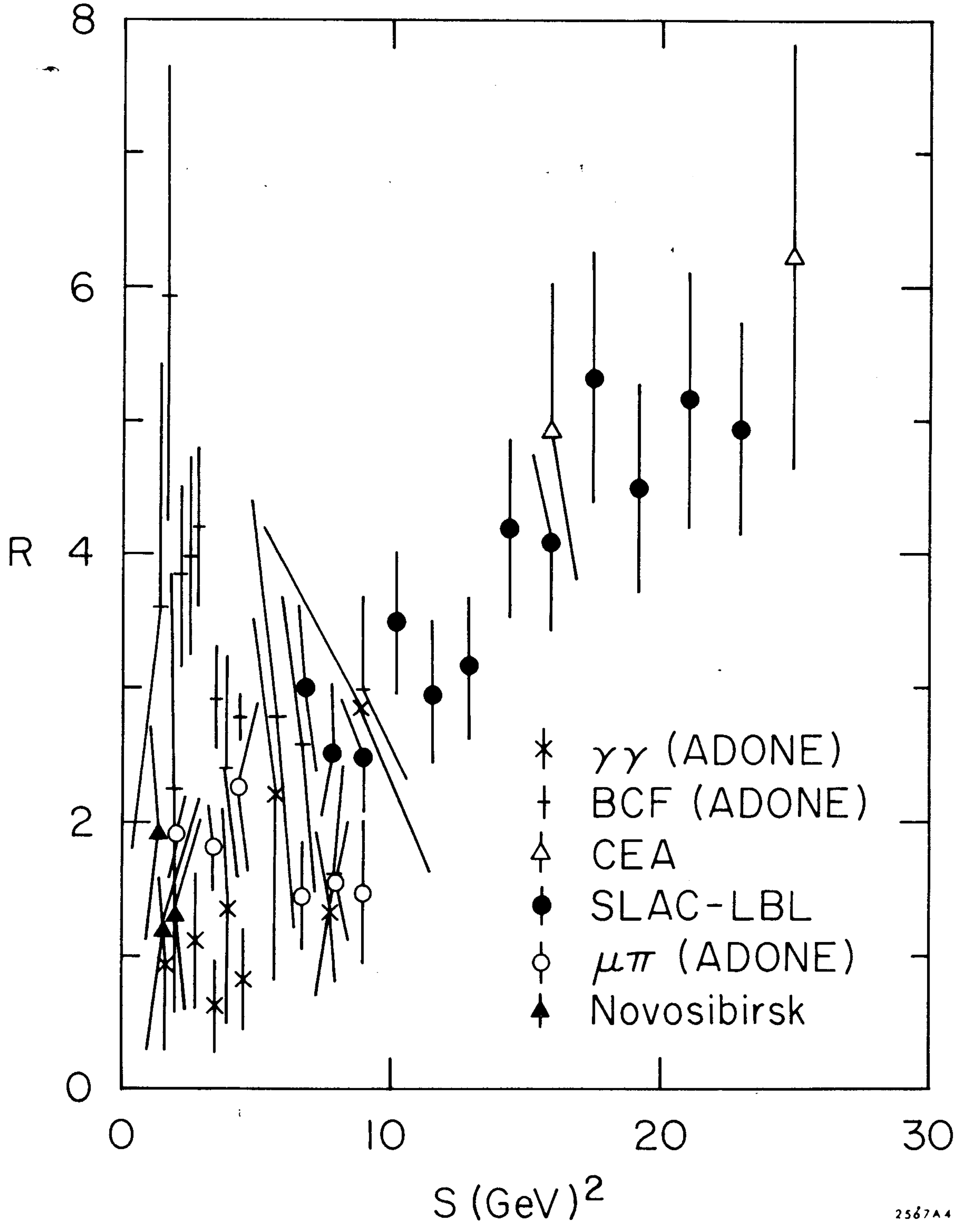

8
6
R 4
2
0
0
10
20
30
S (GeV)^2
γγ (ADONE)
BCF (ADONE)
CEA
SLAC-LBL
μπ (ADONE)
Novosibirsk
2567A4

Fig. 4

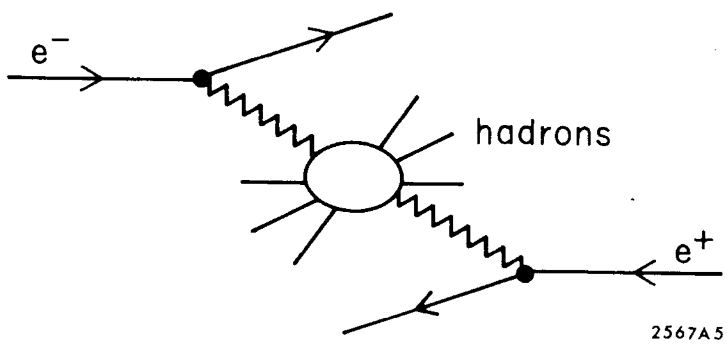

Fig. 5

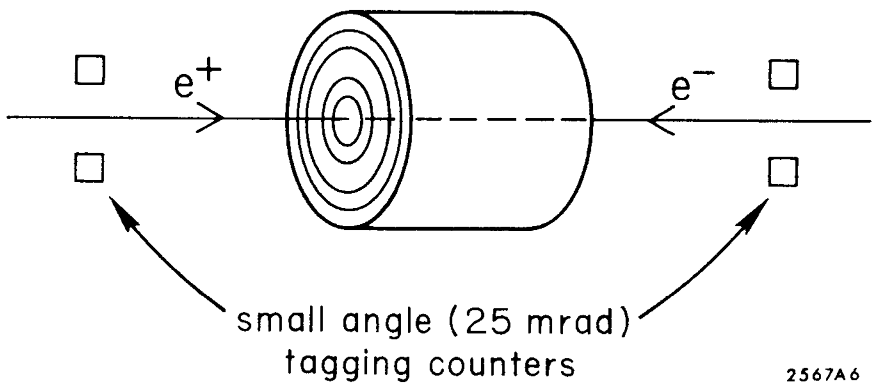

Fig. 6

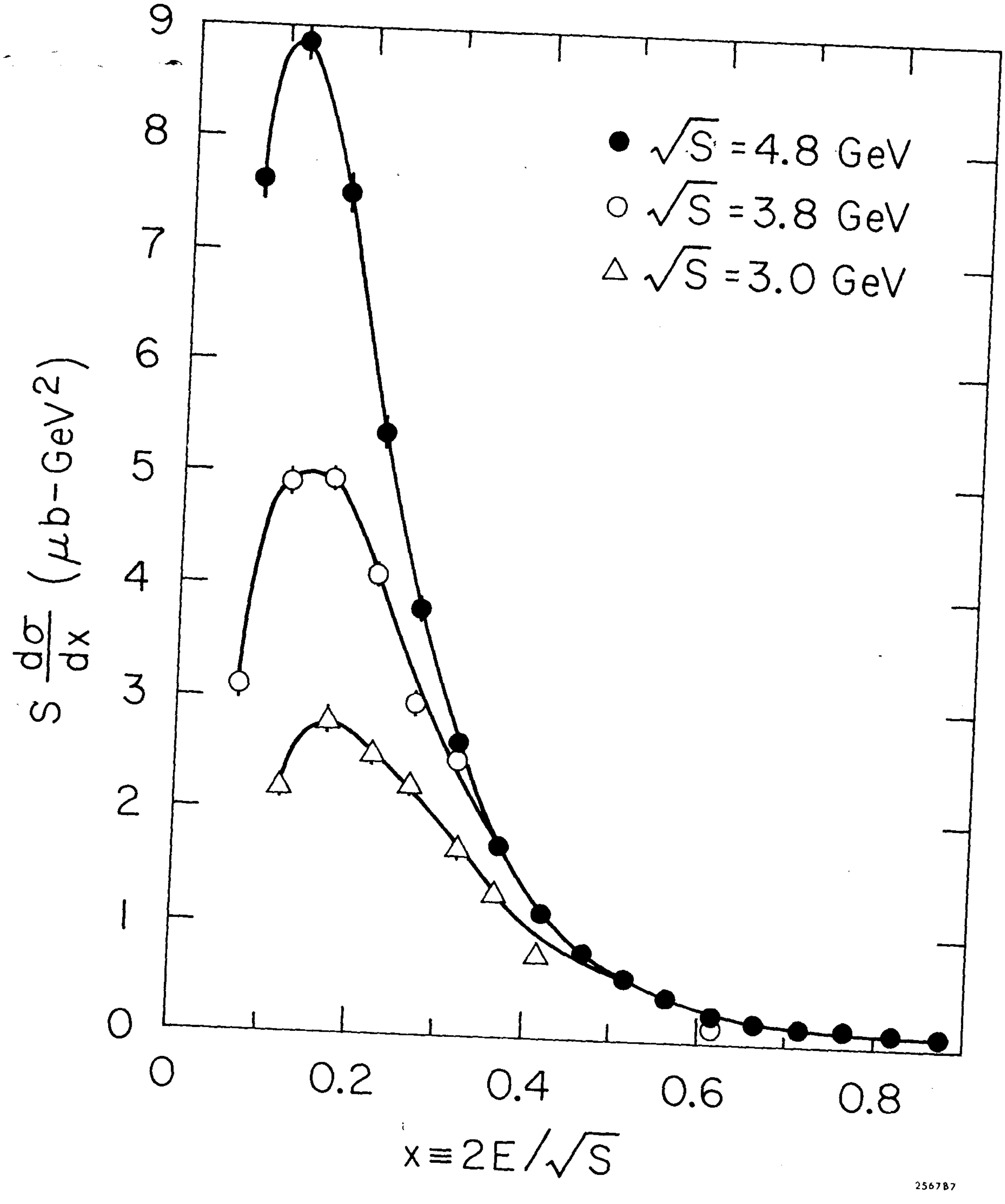

9
8
7
6
5
4
3
2
1
0
0
0.2
0.4
0.6
0.8
$S\frac{d\sigma}{dx}$ (μb-GeV^2)
$x \equiv 2E/\sqrt{S}$
● $\sqrt{S}$ = 4.8 GeV
○ $\sqrt{S}$ = 3.8 GeV
△ $\sqrt{S}$ = 3.0 GeV
2567B7

Fig. 7

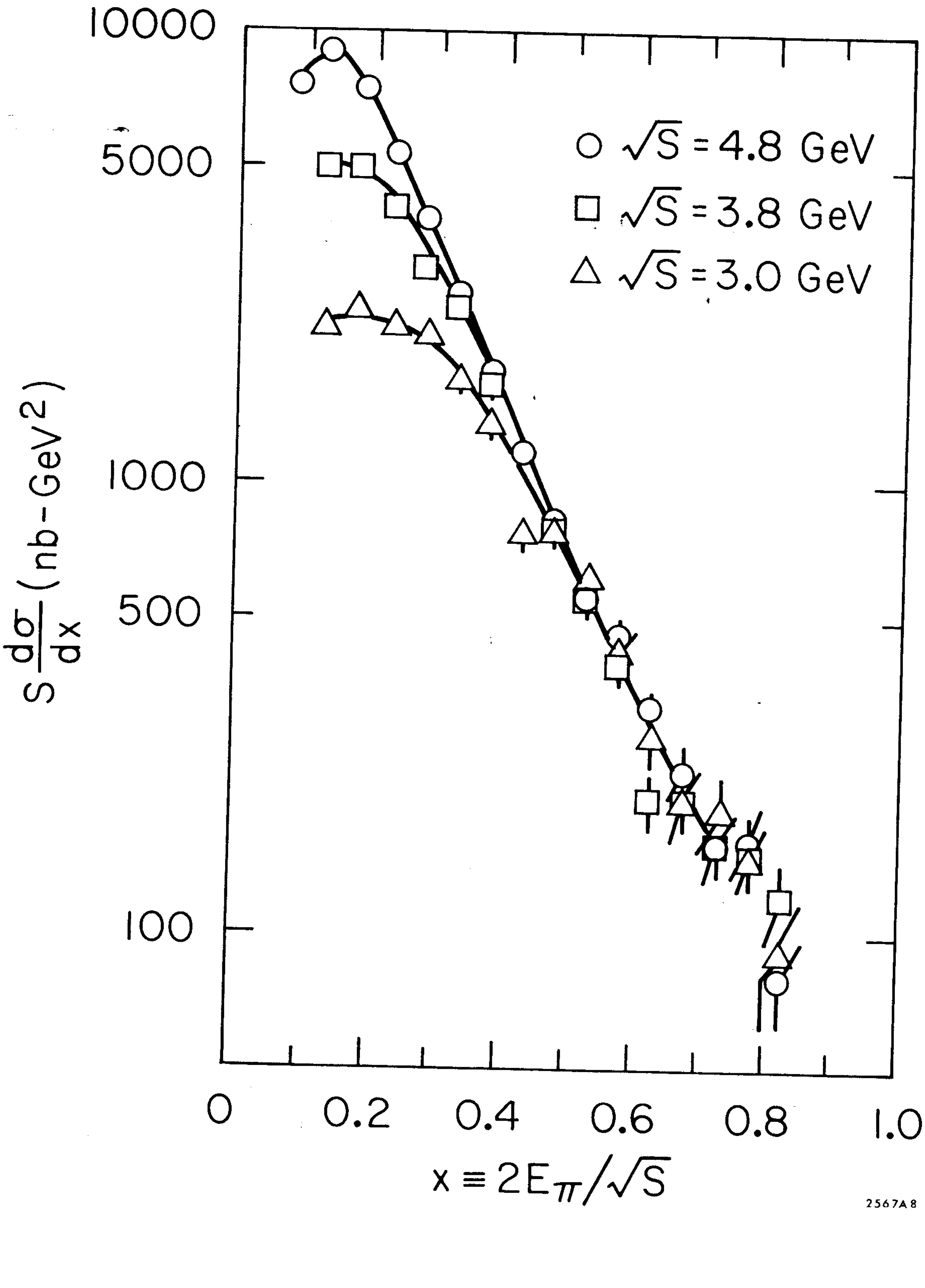

10000
5000
1000
500
100
○ √S = 4.8 GeV
□ √S = 3.8 GeV
△ √S = 3.0 GeV
S dσ/dx (nb-GeV²)
0
0.2
0.4
0.6
0.8
1.0
x ≡ 2Eπ/√S
2567A8

Fig. 8

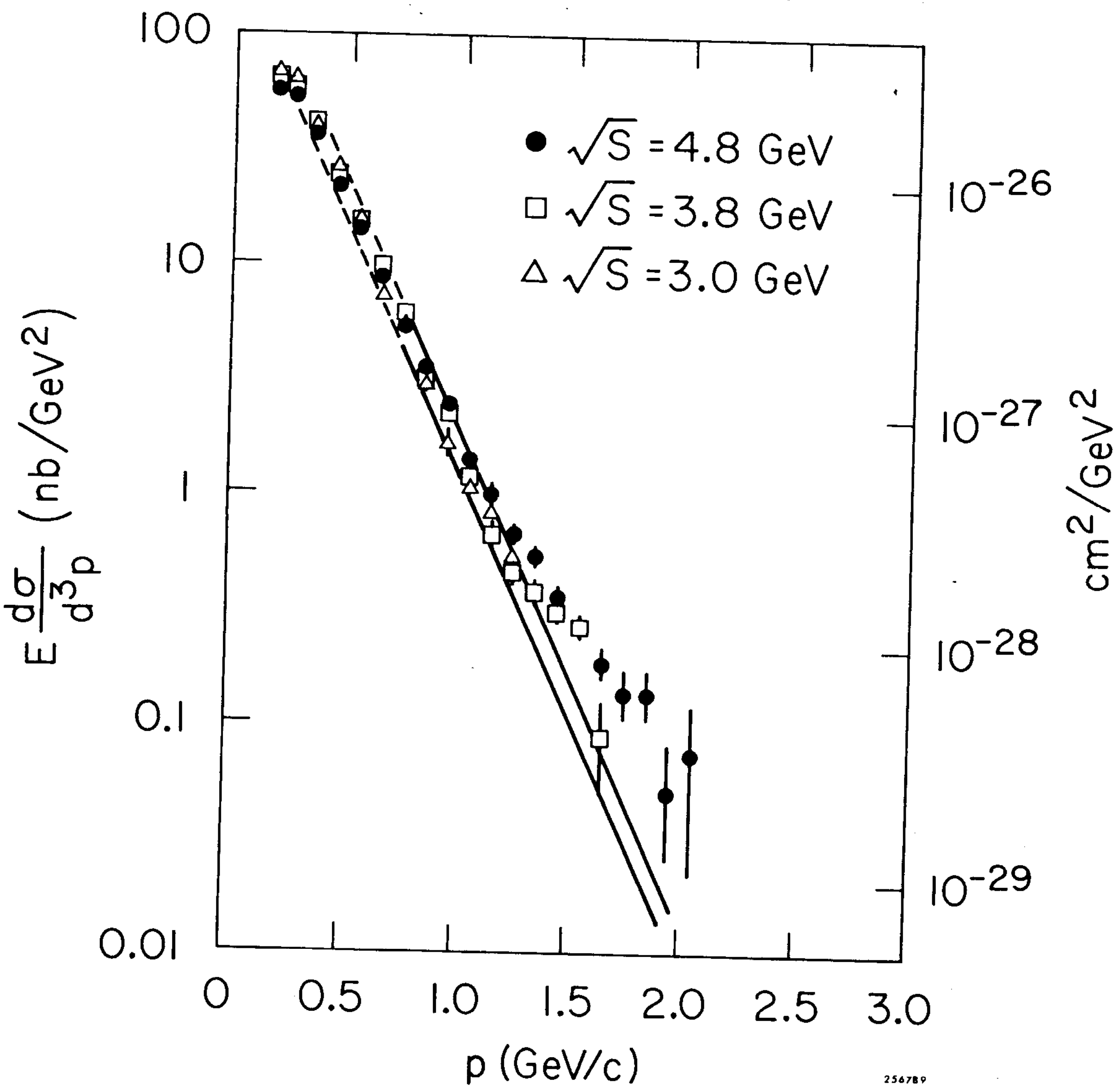

100
10
1
0.1
0.01
10^{-26}
10^{-27}
10^{-28}
10^{-29}
$\sqrt{S}$ = 4.8 GeV
$\sqrt{S}$ = 3.8 GeV
$\sqrt{S}$ = 3.0 GeV
$E \frac{d\sigma}{d^3p}$ (nb/GeV^2)
cm^2/GeV^2
0
0.5
1.0
1.5
2.0
2.5
3.0
p (GeV/c)
256789

Fig. 9

Mean Charged Multiplicity
Preliminary

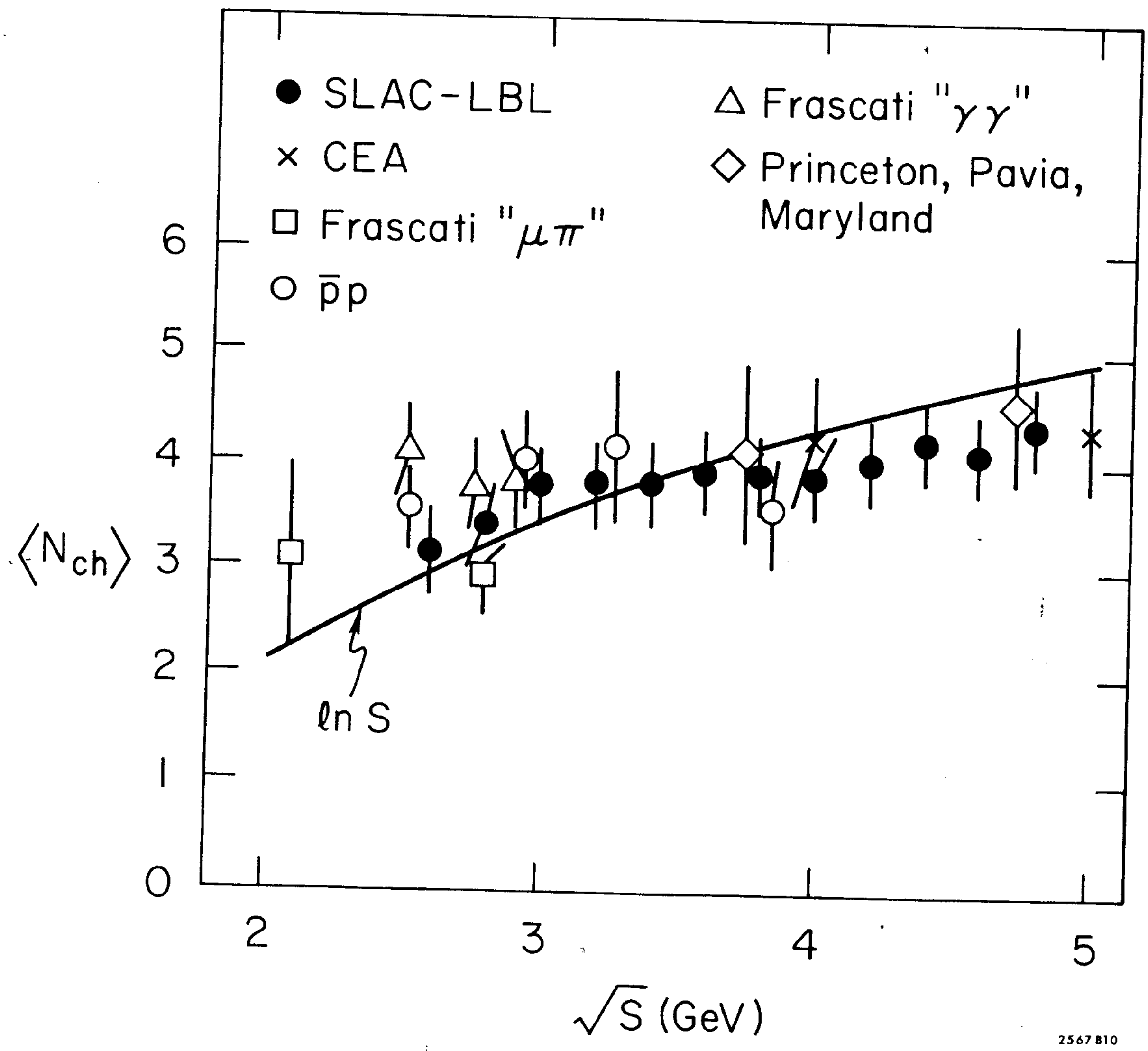

Fig. 10

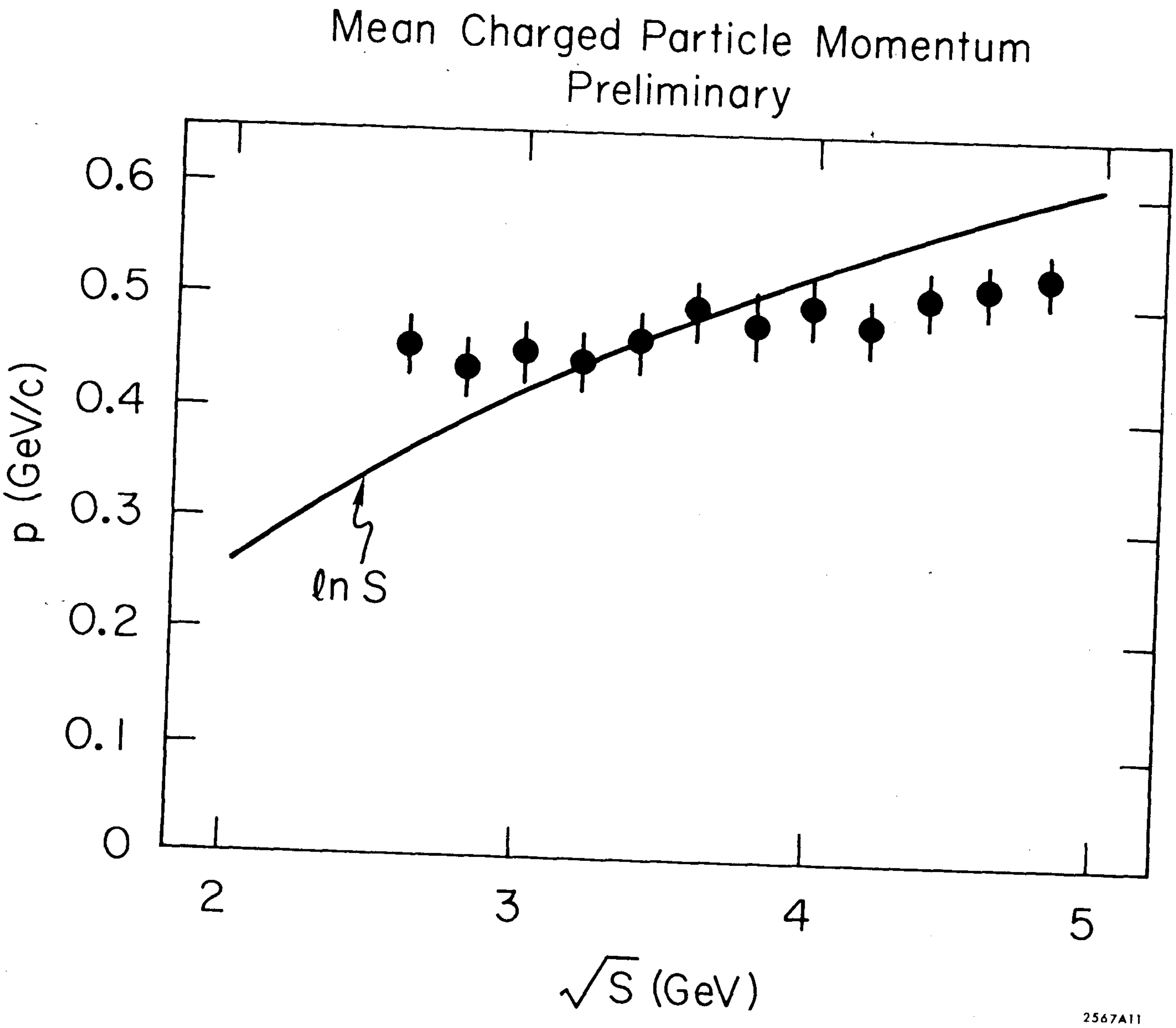
Mean Charged Particle Momentum
Preliminary
p (GeV/c)
0.6
0.5
0.4
0.3
0.2
0.1
0
ln S
2
3
4
5
√S (GeV)
2567A11

Fig. 11

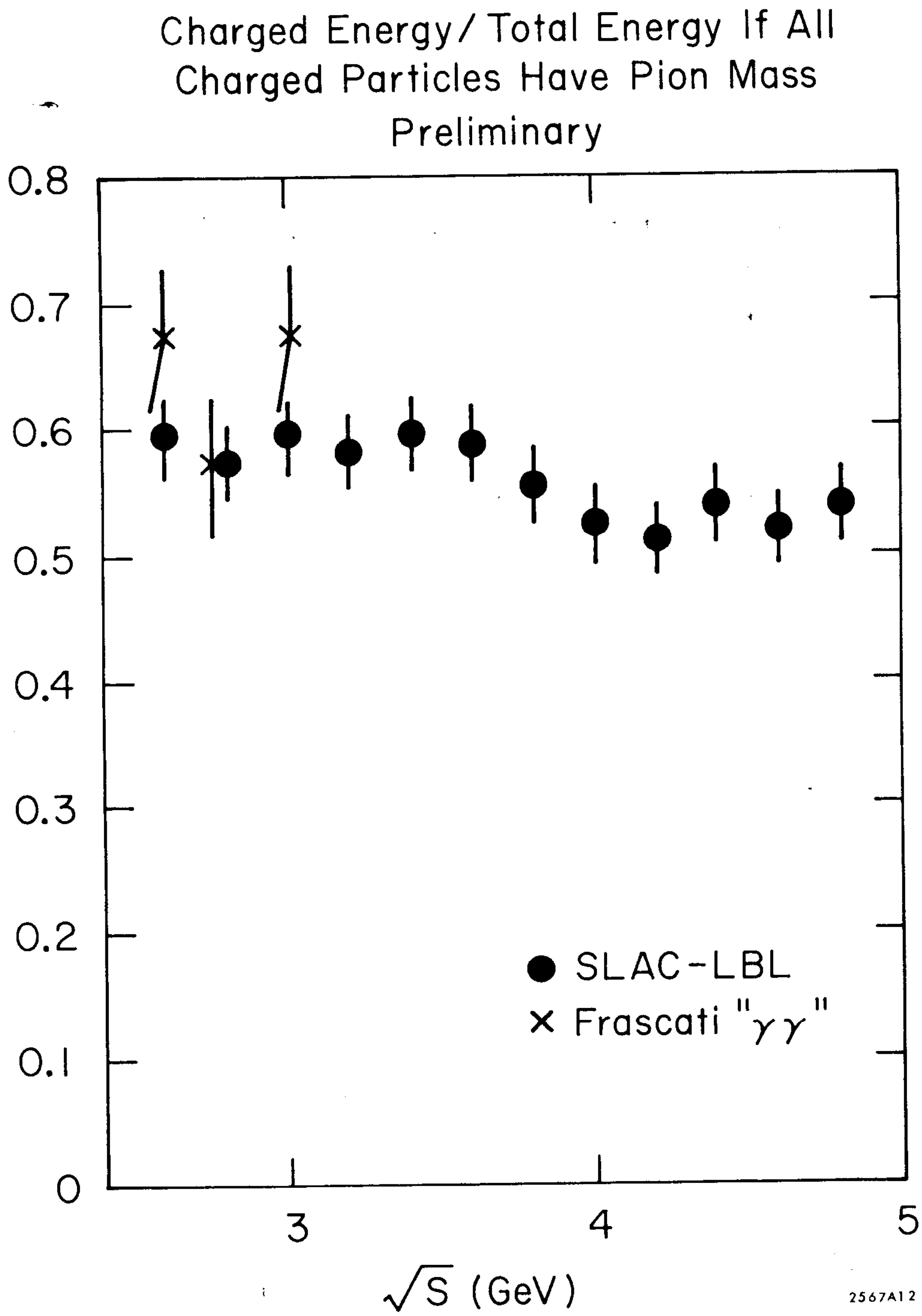
Charged Energy/Total Energy If All
Charged Particles Have Pion Mass
Preliminary
0.8
0.7
0.6
0.5
0.4
0.3
0.2
0.1
0
3
4
5
√S (GeV)
● SLAC-LBL
× Frascati "γγ"
2567A12

Fig. 12

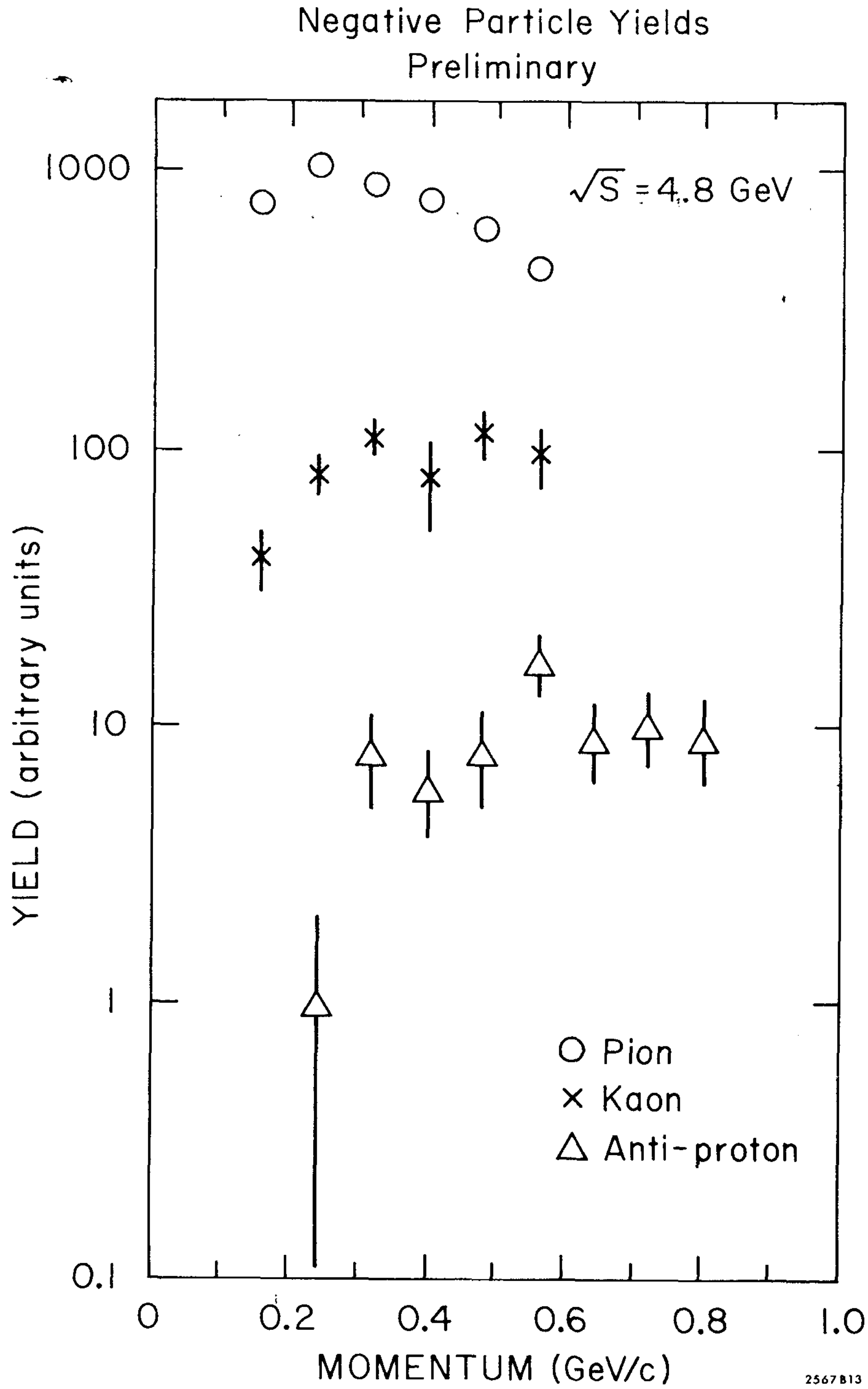
Negative Particle Yields
Preliminary
√S = 4.8 GeV
1000
100
10
1
0.1
YIELD (arbitrary units)
0
0.2
0.4
0.6
0.8
1.0
MOMENTUM (GeV/c)
Pion
Kaon
Anti-proton
2567B13

Fig. 13

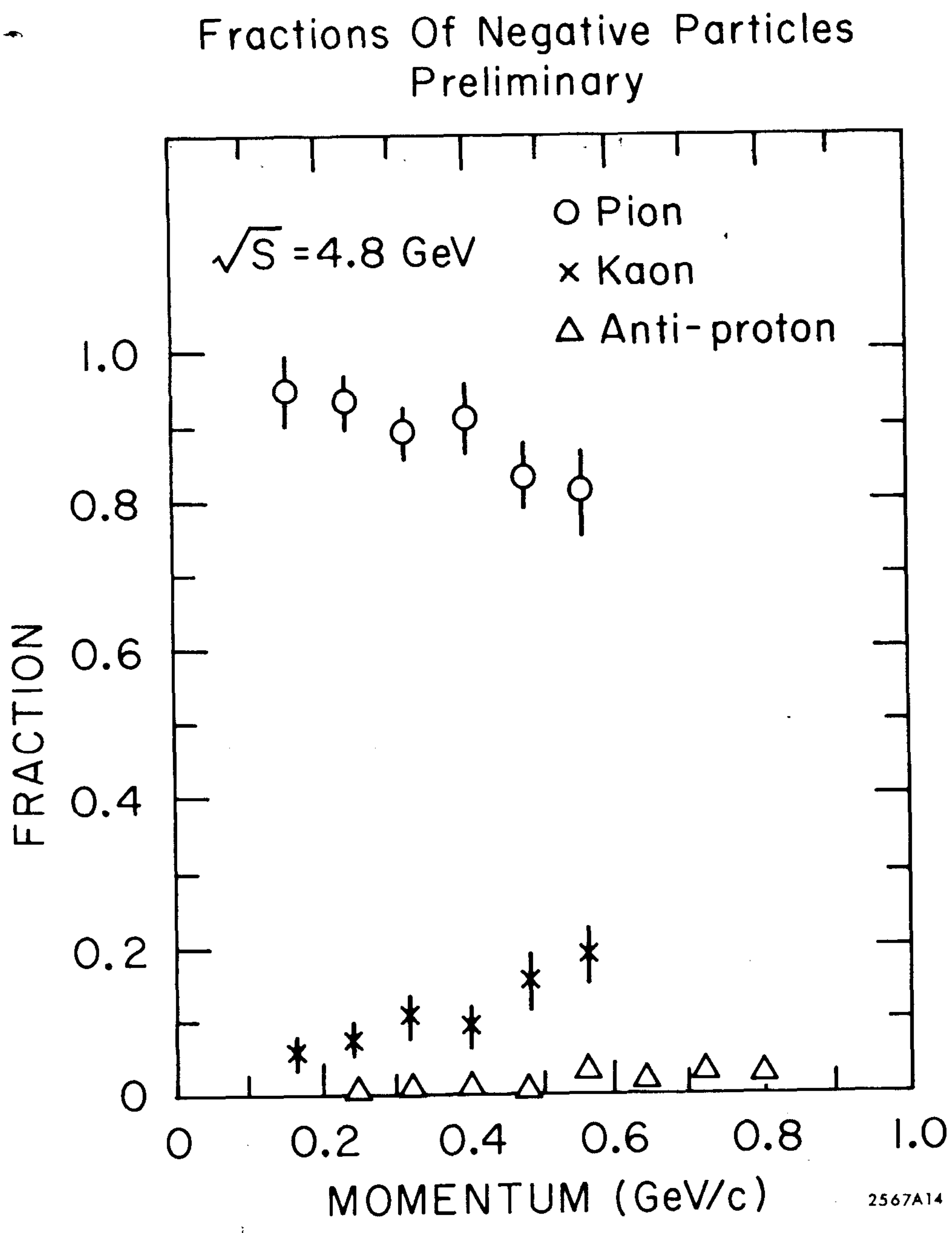

Fractions Of Negative Particles
Preliminary
√S = 4.8 GeV
O Pion
× Kaon
Δ Anti-proton
FRACTION
1.0
0.8
0.6
0.4
0.2
0
0
0.2
0.4
0.6
0.8
1.0
MOMENTUM (GeV/c)
2567A14

Fig. 14

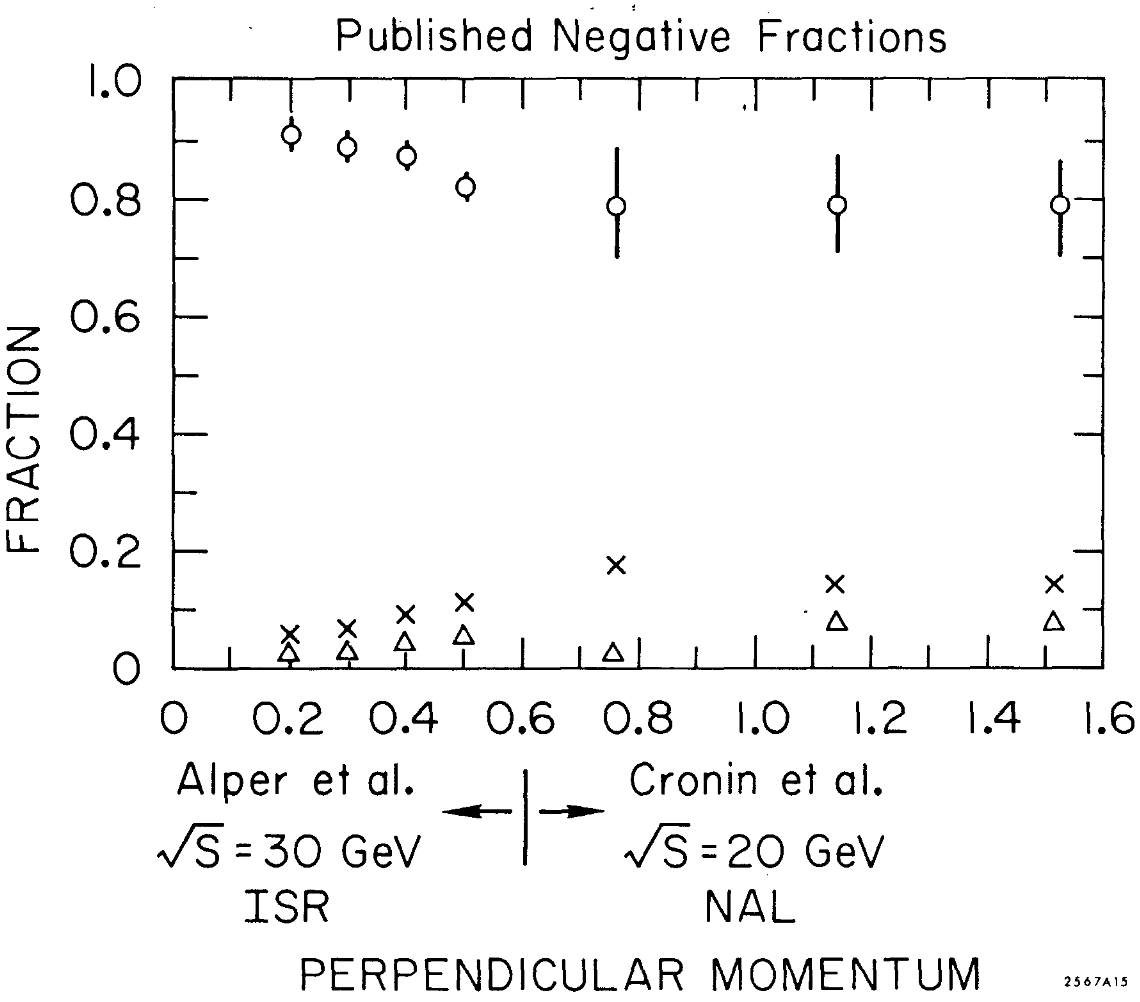

Published Negative Fractions
1.0
0.8
0.6
0.4
0.2
0
FRACTION
0
0.2
0.4
0.6
0.8
1.0
1.2
1.4
1.6
Alper et al.
√S = 30 GeV
ISR
Cronin et al.
√S = 20 GeV
NAL
PERPENDICULAR MOMENTUM
2567A15

Fig. 15

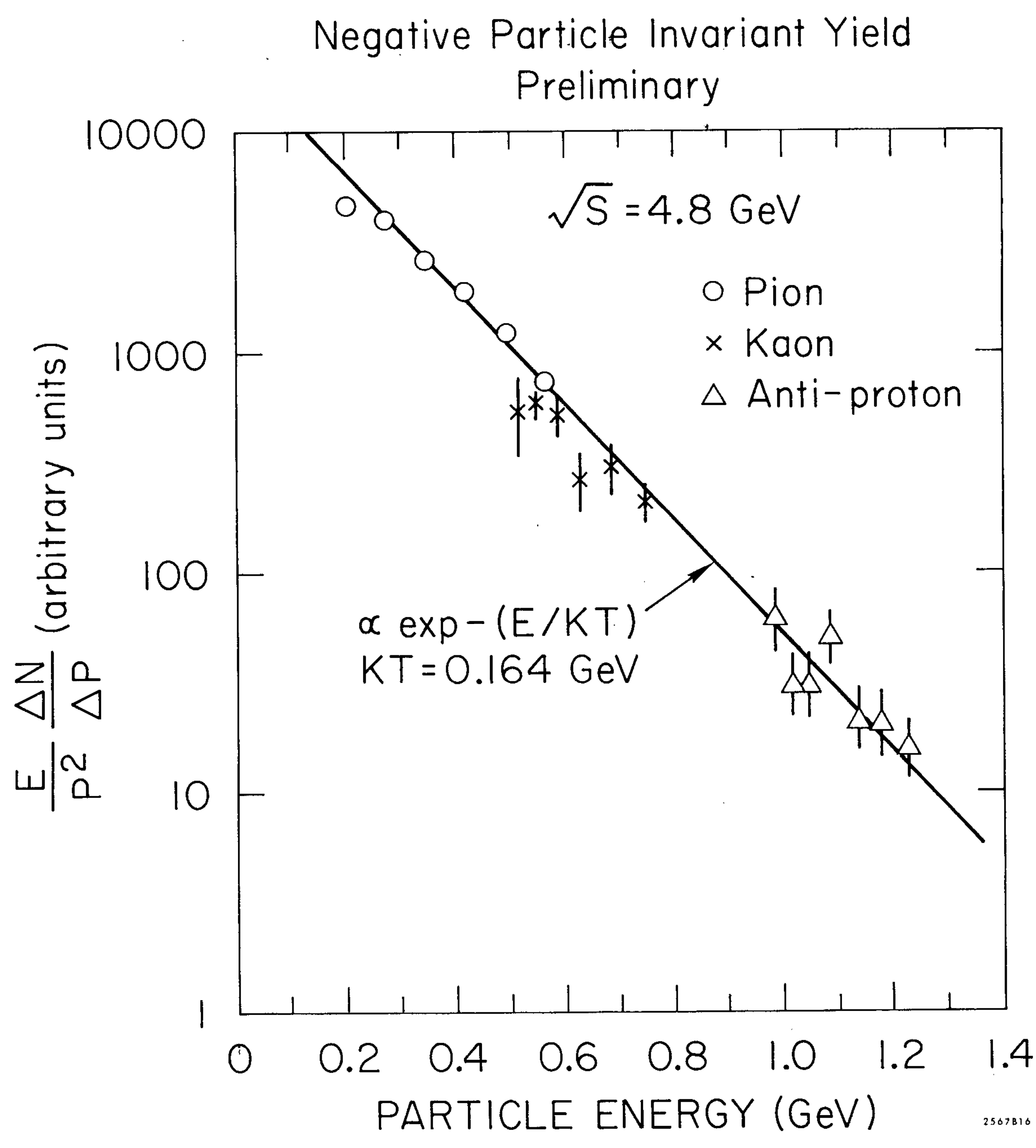

Negative Particle Invariant Yield
Preliminary
√S = 4.8 GeV
○ Pion
× Kaon
△ Anti-proton
α exp-(E/KT)
KT=0.164 GeV
E/P2 ΔN/ΔP (arbitrary units)
10000
1000
100
10
1
0
0.2
0.4
0.6
0.8
1.0
1.2
1.4
PARTICLE ENERGY (GeV)
2567B16

Fig. 16

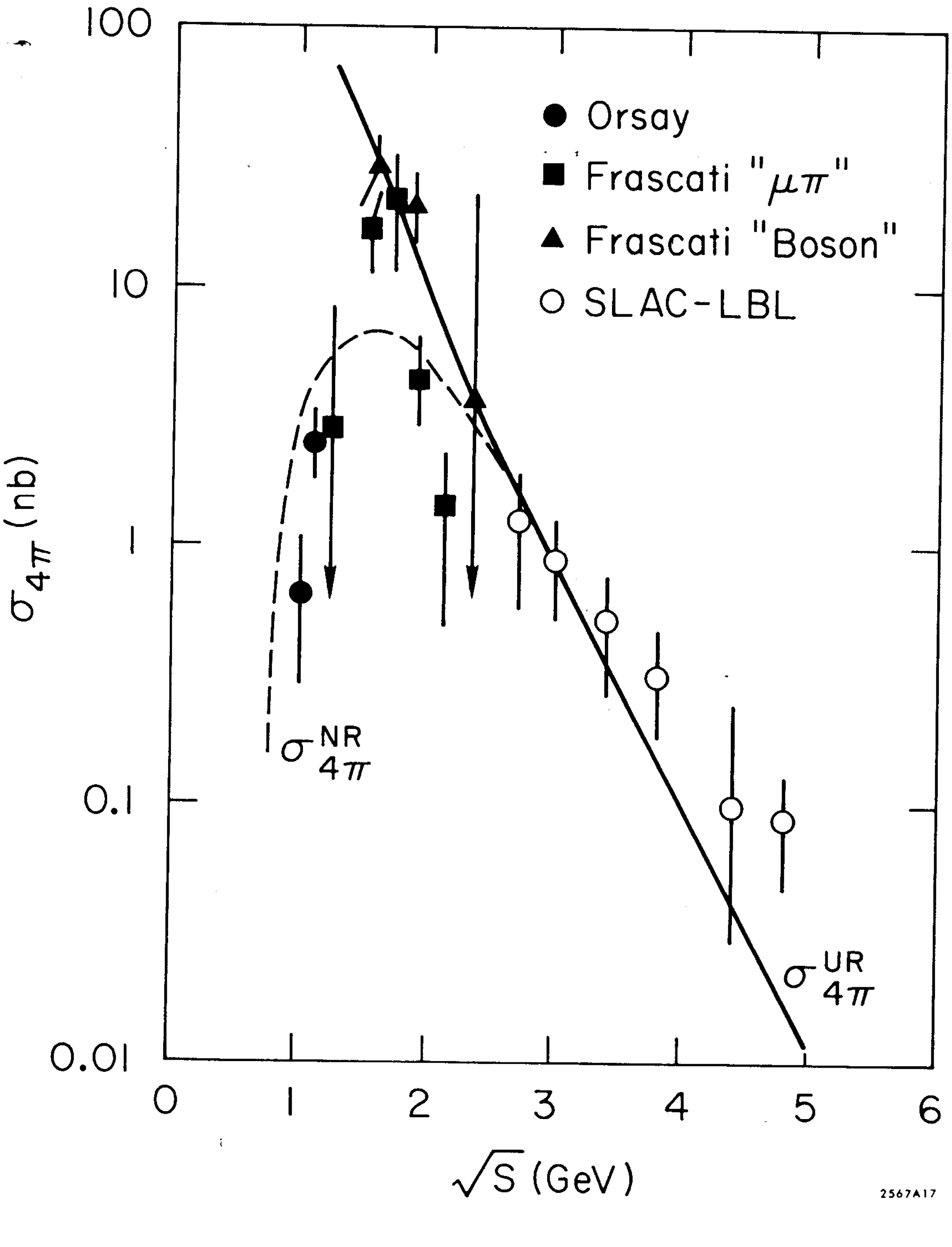
100
10
1
0.1
0.01
$\sigma_{4\pi}$ (nb)
0
1
2
3
4
5
6
$\sqrt{S}$ (GeV)
Orsay
Frascati "$\mu\pi$"
Frascati "Boson"
SLAC-LBL
$\sigma^{NR}_{4\pi}$
$\sigma^{UR}_{4\pi}$
2567A17

Fig. 17

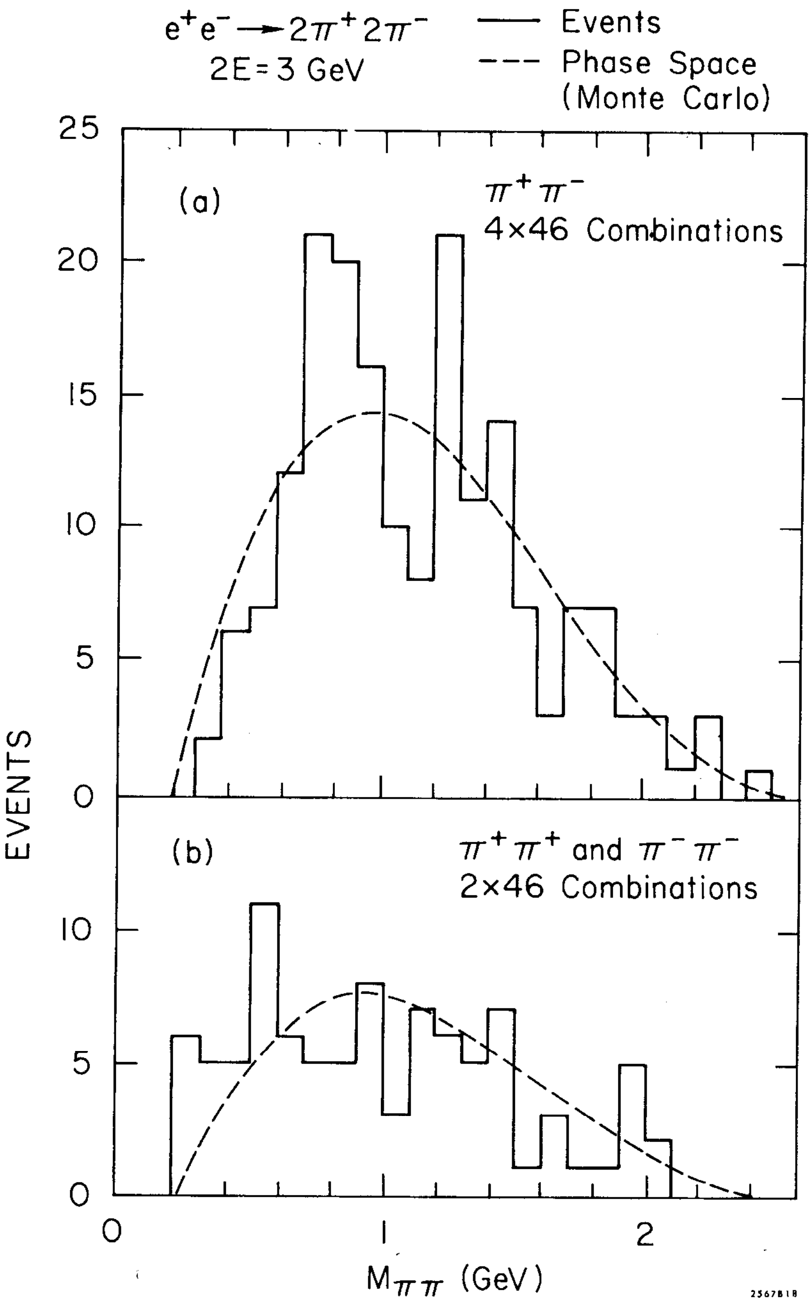

$e^+e^- \rightarrow 2\pi^+2\pi^-$
2E = 3 GeV
Events
Phase Space
(Monte Carlo)
(a)
$\pi^+\pi^-$
4×46 Combinations
(b)
$\pi^+\pi^+$ and $\pi^-\pi^-$
2×46 Combinations
EVENTS
$M_{\pi\pi}$ (GeV)
25
20
15
10
5
0
10
5
0
0
1
2

Fig. 18

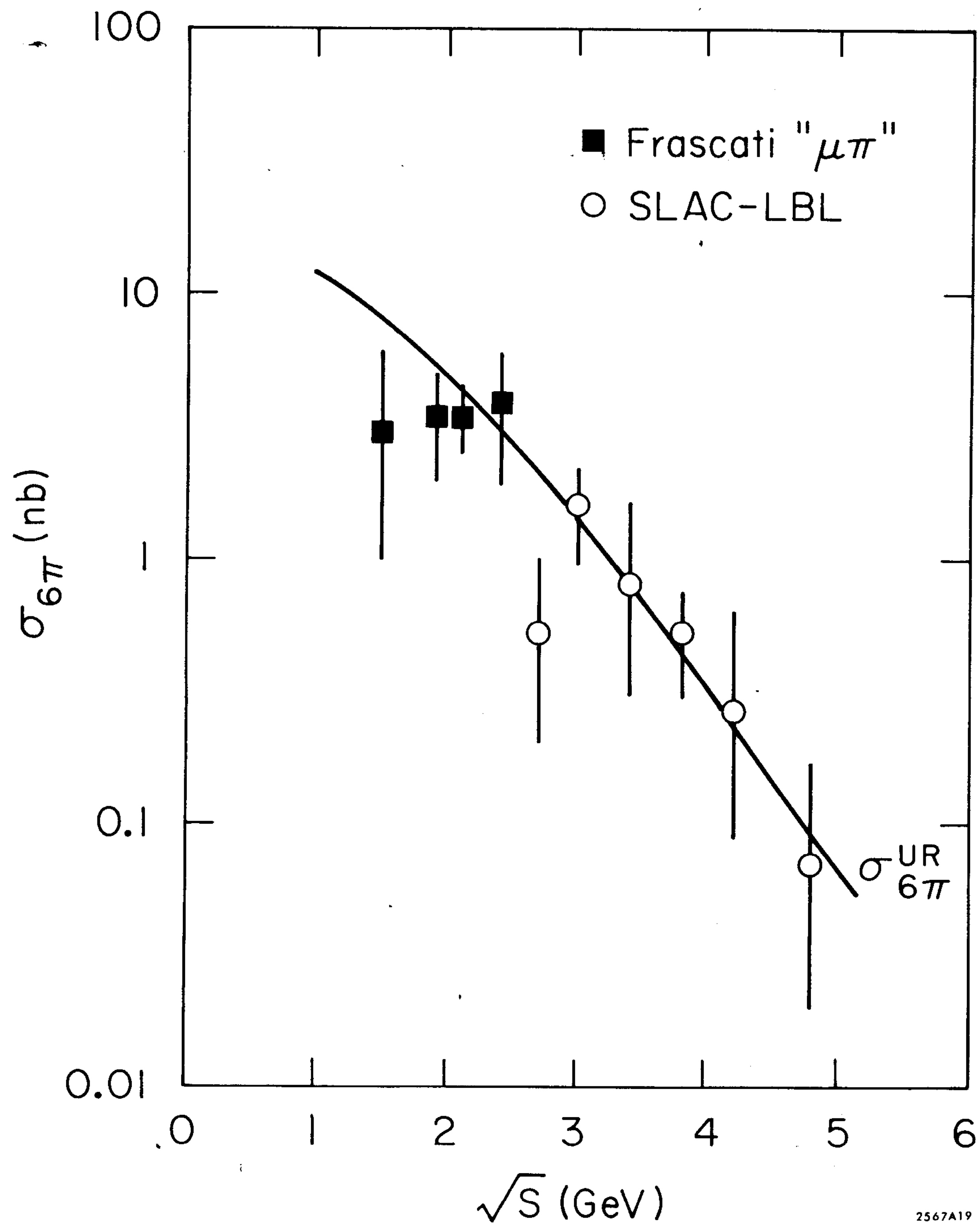

Frascati "μπ"
SLAC-LBL
100
10
1
0.1
0.01
σ6π (nb)
σUR 6π
0
1
2
3
4
5
6
√S (GeV)
2567A19

Fig. 19

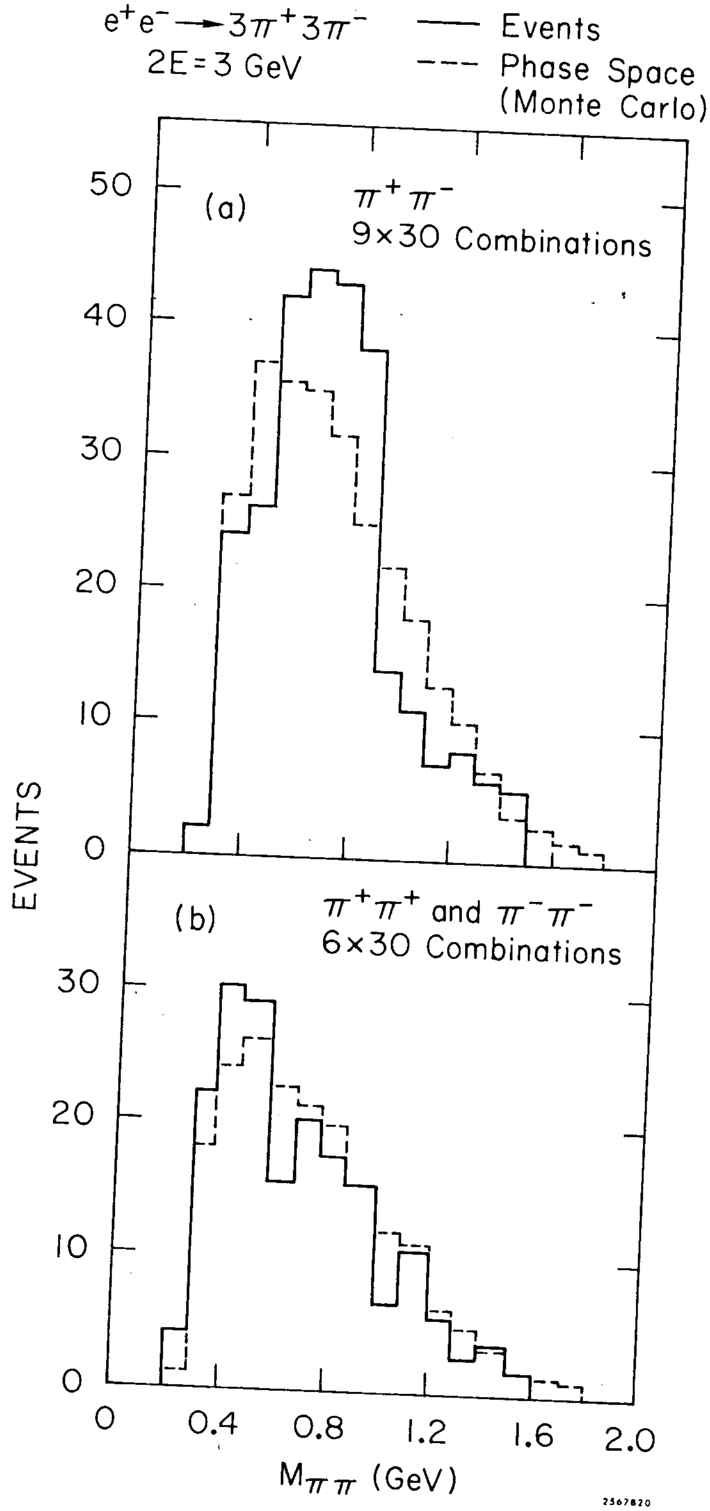
$e^+e^- \rightarrow 3\pi^+3\pi^-$
2E=3 GeV
Events
Phase Space
(Monte Carlo)
(a)
$\pi^+\pi^-$
9×30 Combinations
(b)
$\pi^+\pi^+$ and $\pi^-\pi^-$
6×30 Combinations
EVENTS
50
40
30
20
10
0
30
20
10
0
0
0.4
0.8
1.2
1.6
2.0
$M_{\pi\pi}$ (GeV)
2567820

Fig. 20

$$\begin{pmatrix} p_1 & p_2 & p_3 & \nu_e \\ n_1 & n_2 & n_3 & e^- \\ \lambda_1 & \lambda_2 & \lambda_3 & \mu^- \\ p_1' & p_2' & p_3' & \nu_\mu \end{pmatrix}$$

(a)

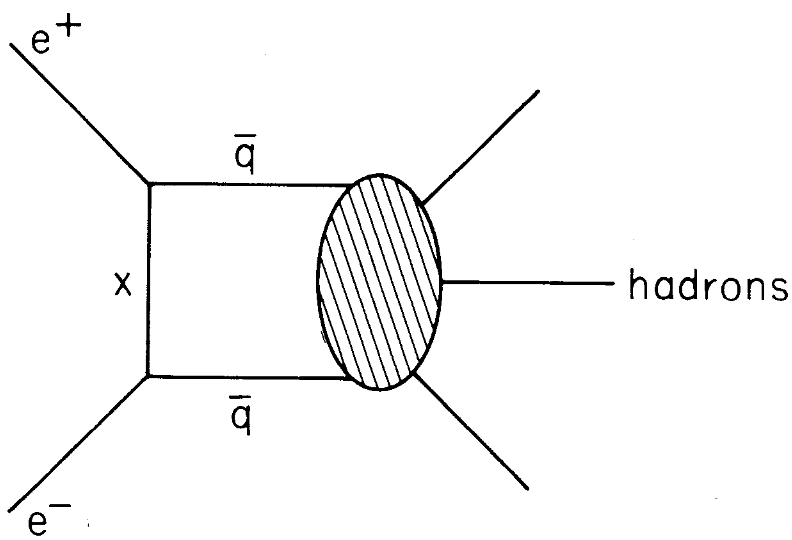

(b)

2567A21

Fig. 21

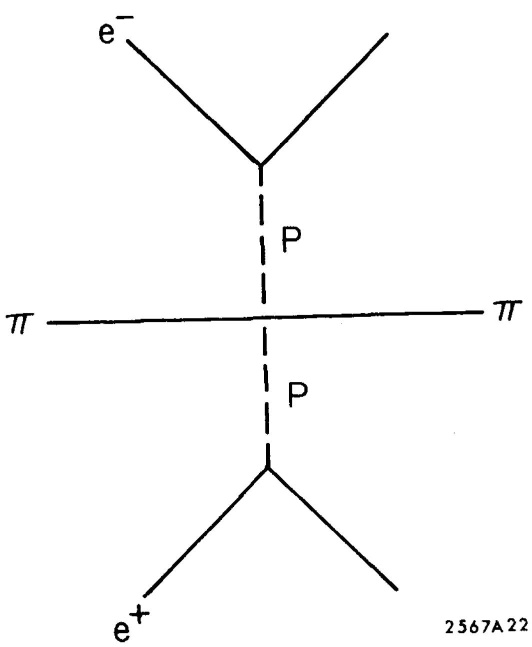

Fig. 22

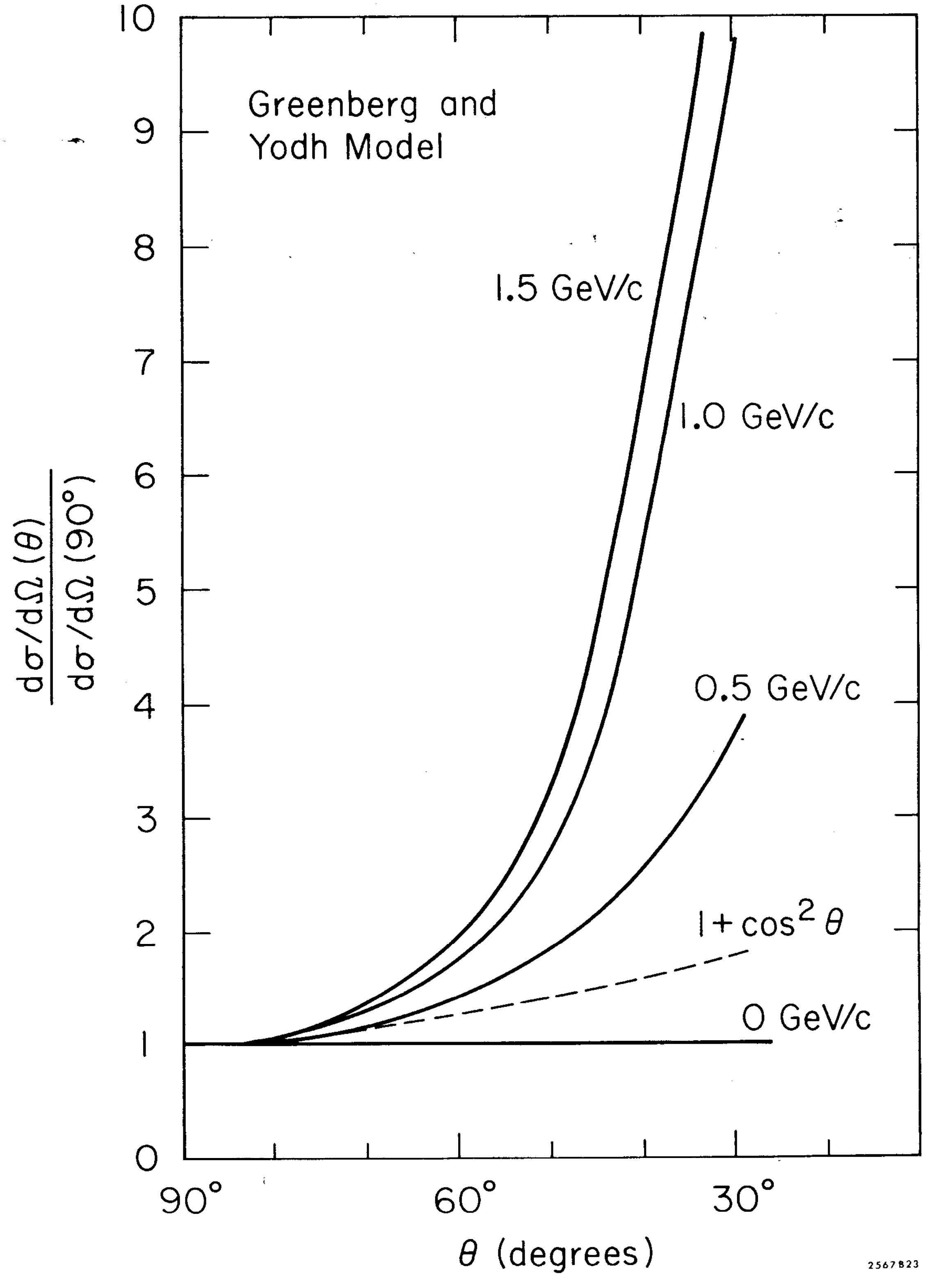
Greenberg and
Yodh Model
1.5 GeV/c
1.0 GeV/c
0.5 GeV/c
1 + cos² θ
0 GeV/c
dσ/dΩ (θ) / dσ/dΩ (90°)
10
9
8
7
6
5
4
3
2
1
0
90°
60°
30°
θ (degrees)
2567B23

Fig. 23

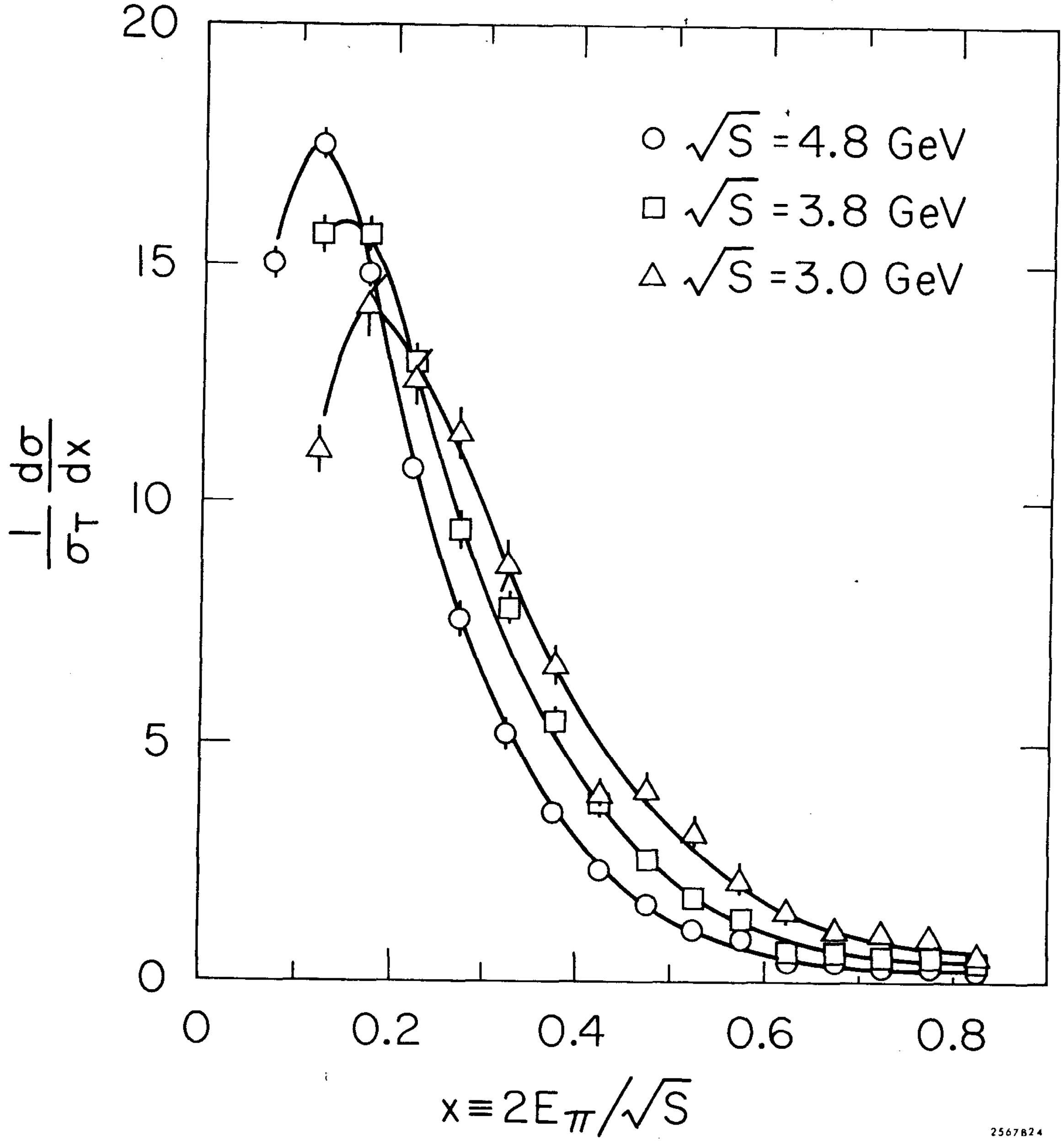

○ $\sqrt{S}$ = 4.8 GeV
□ $\sqrt{S}$ = 3.8 GeV
△ $\sqrt{S}$ = 3.0 GeV
$\frac{1}{\sigma_T}\frac{d\sigma}{dx}$
20
15
10
5
0
0
0.2
0.4
0.6
0.8
$x \equiv 2E_\pi/\sqrt{S}$
2567B24

Fig. 24

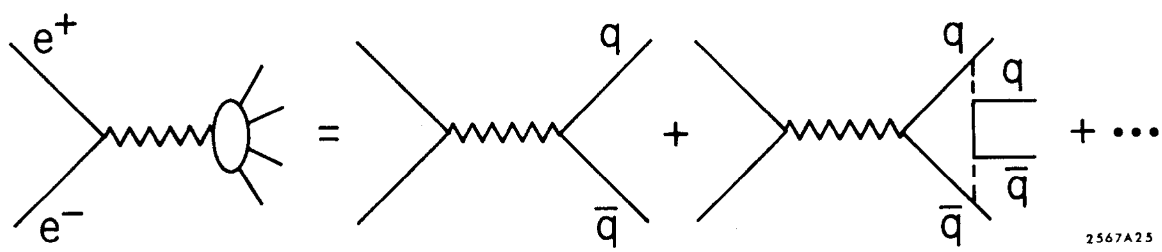

Fig. 25